
Pedalling performance in the BMX supercross gate start

A field-based observational study

Master Thesis
Mechanical Engineering
Biomechanical Design

H.S.J. van Grieken

MSc-thesis advisors: Dr. D.J.J. Bregman
Dr. Ir. A.L. Schwab
Dr. I. Janssen

Delft University of Technology
Faculty of Mechanical, Maritime and Materials Engineering (3mE)
Department BioMechanical Engineering (BMeChE)



Figure 1: Measurement BMX bicycle, photo: Guus Schoonewille, guusschoonewille.nl

Copyright © H.S.J. van Grieken 2019

Author: H.S.J. van Grieken, master student ME at TU Delft. Nothing in this report may be reproduced in any form without written permission.

Abstract

Introduction: In Bicycle Motocross (BMX) racing, a fast gate start is strongly related to overall race performance [1]. Cyclists that lead from the start can choose the most ideal race line and are less likely to get involved in collisions with other competitors. The majority of BMX training is spent on improving physical strength in the gym and bicycle start training to enhance acceleration for a successful start. However, little is known about pedalling characteristics at supramaximal workload levels [2] and instrumentation that meet BMX specific requirements to quantify pedal forces is lacking.

Purpose: The goal of this study was to develop an instrumented BMX bicycle capable of collecting accurate pedal force data during BMX gate start to (1) provide a better understanding of how a cyclist effectively propel the bicycle during a BMX gate start, and (2) identify pedalling variables which are good predictors of a fast gate start.

Methods: Five elite BMX cyclists (male N=3; age 20.7 ± 1.9 yrs, body mass 85.3 ± 6.0 kg; female N=2; age 25 ± 0 yrs, body mass 73.8 ± 4.2 kg) from the Dutch National Team participated in this study. Participants performed six gate starts from a supercross (SX) starting hill (Papendal, Arnhem, The Netherlands) on a test BMX bicycle (Holeshot, Meybo, Boxmeer, Netherlands) equipped with prototype instrumented cranks (Axis2D, Swift Performance, Brisbane, AUS). Pedalling torque and radial force were recorded with 100Hz of both left and right crank independently. Starting performance was defined by the time interval between the gate drop and the cyclist reaching the end of the starting hill (t_{start}). Various strength and technical pedalling variables were calculated from the pedal force data. Variables were analysed using (multiple) linear regression with starting performance.

Results: 60% of the total work (W) by a BMX cyclist is done in the first 5 meters of the start, explaining 91% of variation in starting time ($R^2=90.7$, $p<0.001$). Multiple regression analyses were able to estimate and predict 91.5-93.1% ($F=88.5$, $P<0.001$) and 86.2-89.5% ($F=56.4$, $P<0.001$) of the variation in starting performance from absolute and ratio scaled pedalling variables respectively. The present study revealed that high initial velocity at the gate drop (V_i) in combination with high peak effective force ($F_{e_{max}}$) and power (P_{max}) in the first two pedal strokes and the ability to produce power above 70% of P_{max} over a large crank angle range in the second pedal stroke (Relative Maximum Power Duration, $RMPD_{70}$) are good predictors of starting performance in BMX. Together these variables explain 89-93% of the variation in starting time. Moreover, according to the results of this study time to peak power ($t-P_{max}$), Index of force Effectiveness (IE) and Push Pull ratio (PP) could not be identified as good predictors of performance in BMX racing.

Conclusions: In addition to the previously identified performance predictors, initial velocity and power peak of the first pedal stroke [3], this study reveals that the strength (P_{max}) and technical execution ($RMPD_{70}$) of the second pedal are also an important factors in performing a successful gate start.

Practical applications: A BMX cyclist could (1) focus on an effective slingshot maneuver to increase bicycle velocity at the gate drop, (2) improve maximum power output in the first two pedal strokes and (3) focus on extending the range of high power output in the second pedal stroke, i.e the trail leg. The identified performance predictors P_{max} , Fe_{max} , $RMPD_{70}$ can be quantified without radial force data, meaning instrumentation capable of collection torque and crank angle data alone could be sufficient for performance assessment of the BMX start in daily use.

Contents

Abstract	iii
List of Figures	vii
List of Tables	ix
1 Introduction	1
1.1 Background	1
1.2 Importance of the gate start	3
1.3 Pedalling performance variables	3
1.4 Motivation and research goals	5
1.5 Thesis structure	6
2 Methods and materials	7
2.1 Participants	7
2.2 Environment	7
2.3 Experimental set-up	8
2.4 Procedure	11
2.5 Data processing	12
2.6 Statistical analysis	13
3 Definitions of performance variables	15
3.1 Dependent variable	15
3.1.1 Starting time (t_{start})	15
3.2 General performance variables	15
3.2.1 Velocity at gate drop (V_i)	15
3.2.2 Mass (m)	16
3.2.3 Work (W)	16
3.2.4 Torque peak (T_{max})	16
3.2.5 Power peak (P_{max})	16
3.2.6 Time to power and torque peak ($t-T_{max}$, $t-P_{max}$)	17
3.3 Pedal performance variables	17
3.3.1 Effective force peak (Fe_{max})	17
3.3.2 Resultant force peak (Fr_{max})	18
3.3.3 Power peak per pedal stroke	18
3.3.4 Relative Maximum Power Duration ($RMPD_{90}$, $RMPD_{70}$)	18
3.3.5 Index of force Effectiveness (IE)	18
3.3.6 Push Pull ratio (PP)	18

3.3.7	Dead center size (<i>DC</i>)	19
4	Results	21
4.1	Movement phases	21
4.2	Crank data	22
4.3	Propulsion	25
4.3.1	Pedal forces	25
4.3.2	Torque-cadence profile	26
4.3.3	Power-velocity profile	26
4.4	Work	28
4.5	Performance variables	30
4.5.1	General variables	30
4.5.2	Peddalling variables	32
4.6	Participants subjective performance assessment	38
5	Discussion and implications	41
5.1	Ecological validity	42
5.2	Comparison with other literature	45
5.3	Limitation	47
5.4	Practical relevance	47
6	Conclusion	49
6.1	Conclusion	49
6.2	Practical application	49
6.3	Recommendations and future outlook	49
7	Acknowledgement	51
A	Description and specifications of the instrumented cranks	57
A.1	Product description	57
A.2	Gain and Offset compensation	58
A.3	Data processing	59
B	Wheel velocity sensor	61
B.1	Hardware	61
B.2	Software	62
C	Figures of results	67
C.1	Cumulative work figures	67
D	Regression model details	71

List of Figures

1	Measurement BMX bicycle photo:guusschoonewille.nl	ii
1.1	BMX track Arnhem, The Netherlands	2
1.2	BMX bike	2
1.3	Movement phases	3
2.1	Diagram of BMX supercross ramp	8
2.2	Instrumented BMX bicycle equipped with multiple sensors.	9
2.3	Schematic drawing of instrumented cranks	10
2.4	VAS score leaflet example	12
3.1	Crank revolution sections and pedal forces	17
4.1	Example recording from Axis2D instrumented cranks	23
4.2	Example corrected data from Axis2D instrumented cranks	24
4.3	Pedal forces	25
4.4	Example Torque-Cadence profile	26
4.5	Example Power-Velocity profile	27
4.6	Cumulative work per trial for one participant	28
4.7	Mean cumulative work done per rider	29
4.8	Relationship between general variables and starting time	31
4.9	Relationship between pedalling variables and starting time (1)	33
4.10	Relationship between pedalling variables and starting time (2)	34
4.11	Effective force of the first crank revolution	38
4.12	Relationship between VAS score of participants and starting time	39
5.1	Crank revolution sections	44
A.1	Axis2D Swift performance system	57
B.1	Custom speed sensor	62
C.1	Rider 1 cumulative work	67
C.2	Rider 2 cumulative work	68
C.3	Rider 3 cumulative work	68
C.4	Rider 4 cumulative work	69
C.5	Rider 5 cumulative work	69
D.1	Normal probability plot, General variables, Absolute power data	71
D.2	Normal probability plot, General variables, Absolute work data	72

D.3	Normal probability plot, General variables, Ratio scaled data	73
D.4	Normal probability plot, pedalling variables, absolute data	74
D.5	Normal probability plot, pedalling variables, absolute data using power	75
D.6	Normal probability plot, pedalling variables, ratio data	76
D.7	Normal probability plot, pedalling variables, ratio data with power	77

List of Tables

2.1	Descriptive data of participants	7
2.2	Dimensions of the BMX supercross start ramp (Arnhem, Papendal) used for experiments	8
2.3	Movement phases of the BMX gate start	11
2.4	Pearson correlations for scaled strength related variables	14
4.1	Movement phase times per rider	21
4.2	Movement phase time per group	22
4.3	Work done per section of start hill	30
4.4	Work portion of energy input	30
4.5	Descriptive data general variables	32
4.6	Descriptive data strength pedalling variables (1)	35
4.7	Descriptive data technical pedalling variables (2)	36
A.1	Twist compensation coefficients	58
A.2	Calibration settings crankset	59
A.3	Hardware specifications on Axis2D instrumented cranks	59
D.1	Multiple regression analyses of general variables, for power peak	71
D.2	Multiple regression analyses of general variables, for work	72
D.3	Multiple regression analyses of ratio scaled general variables, for work	73
D.4	Multiple regression analyses of pedalling variables	74
D.5	Multiple regression analyses of pedalling variables using power	75
D.6	Multiple regression analyses of ratio scaled pedalling variables	76
D.7	Multiple regression analyses of ratio scaled pedalling variables using power	77

Chapter 1

Introduction

The goal of this study is to (1) provide a better understanding of how a cyclist effectively propel the bicycle during a Bicycle Motocross (BMX) gate start, and (2) identify pedalling variables which are good predictors of a fast gate start. The focus of this project was prompted by discussions with members of Royal Dutch Cycling Union, who wants to know, in general, what defines a 'optimal' BMX gate start and how they could use pedal force measurement during training. This thesis is a report of field-based measurements during the BMX start of world class athletes on a UCI standard BMX Supercross (SX) starting hill.

Out of the 38 world-championship cycling events governed by the Union Cycliste Internationale (UCI) 24¹ are often decided in a sprint [4]. So sprint performance is a major determinant of most world-championship cycling events. One of those sprint cycling events is BMX racing, where races are defined as all-out sprint efforts.

1.1 Background

From the late 1960's children were inspired by the motocross sport in California, USA. On their bicycles they raced each other on self-made dirt tracks. This was the beginning of what now has become a full grown professional sport, BMX racing. After its introduction in the 2008 Olympic Games (Beijing, China) BMX racing has established a solid position within the cycling sport. The format of BMX racing consists of heats where cyclists compete to qualify for the next round to eventually progress to the final race. A BMX heat is a mass-start bicycle race lasting 35–45 seconds where a maximum of 8 cyclists contest over one single lap on a dirt track (300-400m in length) with jumps, bends, and obstacles. Figure 1.1 shows the BMX Supercross track at Papendal, Arnhem, home track of the Dutch National Team and host of several WorldCup events. BMX SX is the Olympic category in which the start gate is positioned on top of a 8 meter high start hill, where cyclists develop the majority of the velocity they need for the rest of the race. The geometry of the start hill is the same for every BMX SX track, the dirt track layout differs for every track.

¹From five disciplines combined, (1)Road, (2)Track, (3) Cyclo-cross, (4)MTB and (5) BMX. , 10 are all-out sprints (men's and women's sprint, 500/1000 m time trial, Keirin, four-cross and BMX), 10 are often decided in the finish sprint (men's and women's road race, scratch, XC, XCE, marathon) and 4 require repeated sprints (men's and women's point race, omnium).



Figure 1.1: BMX track at Sport Centre Papendal, Arnhem, The Netherlands. Photo adopted from papendal.nl 2019.

BMX cyclists ride on 20 inch bicycles (see Figure 1.2), wear full face helmets and protective gear. The bicycle has a single speed freewheel hub drivetrain and the frame is typically made of aluminium. Racing tires are relatively wide with a low-profile to increase traction on the dirt track but minimize rolling resistance and are typically inflated up to 6 bar. The cyclists clip their shoes into the pedals, ensuring their feet are always in contact with the pedals and enables the abilities to push and pull on the pedals. The saddle is mandatory [5], but cyclists remain in a standing position the entire duration of the race.



Figure 1.2: A BMX bicycle (Holeshot, Meybo, Boxmeer, The Netherlands). Photo adopted from meybobikes.com 2018

BMX cyclist perform a standing start from the gate. After a random delay, (between 0.1 seconds and 2.7 seconds) three LED lights and pulse tones are activated (taking 0.360 seconds) before the gate drops. Cyclists are allowed to move before the gate drop. Kalichová et al. [6] defined five movement phases for the gate start (see Figure 1.3). The preparation movements and part of the first pedal stroke are performed before the gate drops. This “slingshot” maneuver is used to maximize the initial forward velocity of the bicycle [7]. Cyclist pull up the front wheel during this maneuver and ride a certain part of the start on the rear wheel only.



Figure 1.3: A gate start performed by a cyclist of the Dutch national team, split in the five movement phases defined by Kalichová et al. [6]

1.2 Importance of the gate start

The start is the most crucial part of a BMX race. Cyclists that lead from the start are less likely to make contact with competitors which could result in collisions, moreover they can choose the most ideal line into the first jump, first turn and dictate the rest of the race, according to coaches and athletes. The majority of training is spent on improving physical strength in the gym and bicycle start training to enhance acceleration for a successful start. A leading position (1st to 3th) gained after the start (8-10 seconds in the race) has a strong correlation with a top three placement on the finish line concluded Rylands & Roberts after analysing 175 BMX SX races by [1]. Zabala et al. [7] studied the effect of feedback in an intervention with the Spanish national team cyclists (n=6) conducting specific gate start training which led to significant improvements in gate start time (in the order of 100-200ms). The participants reported improvements in their results in the following international competitions mainly due to the improvement in their start position, underlining the importance of the start to overall performance.

1.3 Pedalling performance variables

Strength related variables

Cowell et al. [8] took a closer look at the pedalling contribution in this part of the race and revealed that the majority of the time was spent pedalling (78% and 60% of the time for men and women respectively), showing the importance of the pedalling action in the part of a

race. Developing maximum mechanical power and torque (P_{max} [W] and T [Nm] respectively) are determining performance factors for BMX cyclist on levelled ground sprints [9] and on a starting ramp [3]. In the Olympic BMX SX races elite cyclists are able to reach peak power (> 2000 Watt) and cadence ($> 200 \text{ rev} \cdot \text{min}^{-1}$) within 6.0 meters and 1.6 seconds (Herman et al., 2009 [10]) [8]. In a sport where success and failure are within the margin of 1%, even small performance enhancements at the start would allow an cyclist to obtain an advantageous position to lead the race [11].

Potential technical related variables

Analysing technical pedaling variables in sprinting is quite novel. Four potential technical variables for BMX application are identified from literature. A full description of all used variables in this study can be found in Chapter 3.

Index of Effectiveness

The first and most used measure of technique in cycling is pedal force effectiveness and can be quantified by the Index of Effectiveness (IE) [2]. This mechanical effectiveness is defined as the ratio of the tangential crank force (i.e. the effective force) to the total force applied to the pedal (i.e. the resultant force) over one crank revolution. A recent study by Janssen & Cornellisen [12] found significant differences in IE between track and BMX cyclists during laboratory-based ergometer sprints.

Relative Maximal Power Duration

The second technical pedalling variable is Relative Maximal Power Duration ($RMPD$ [$^{\circ}$]) introduced by Bertucci et al. [13] and quantifies a cyclist ability to produce instantaneous power above 90% ($RMPD_{90}$) or 70% ($RMPD_{70}$) of the P_{max} over a large crank angle interval. The variable revealed that elite cyclo-cross cyclist are able to generate higher power outputs over a large range of crank angles compared to regional cyclists in stationary ergometer sprints.

Dead Center size

The third technical variable is Dead Center size (DC) and provides information on a cyclists ability to overcome a crank position where it is seemingly very difficult to produce high power output; at the top and bottom of the crank cycle, Top Dead Center (TDC) and Bottom Dead Center (BDC) respectively. DC is defined as the pedal work rate in these difficult sections compared to the average work rate through a crank cycle. DC is an important trait of pedaling during sub-maximal ergometer cycling [14]. Translating to standing starts; the more even the crank cycle is in the dead center, the lower the repetitive deceleration of a cyclists inertia during the sprint, which might be beneficial during BMX gate starts.

Push Pull ratio

Lastly, the Push Pull ratio (*PP*) provides information and the contribution of pulling on the pedal during the upstroke of the crank cycle to the total torque production. *PP* is defined as the ratio of pulling force to the total force over a pedal stroke. An active pull increases the mechanical effectiveness of pedalling in sub-maximal ergometer tests [15].

These laboratory based results of four technical variables provide an indication of pedalling performance and reason for further investigation into BMX gate start performance.

1.4 Motivation and research goals

Over the years, numerous studies have investigated pedalling performance in cycling. Yet, these studies have been focused on endurance cycling at sub-maximal workload levels in laboratory controlled trials, rather than sprint performance in race environment. Little is known about pedalling characteristics at supramaximal workload levels [2]. Since BMX racing has become an Olympic discipline it has raised more attention in research. Nevertheless, the number of performance characteristic studies in BMX is limited [16]. Furthermore, two issues can be identified in the studies that investigated the physical performance of BMX cyclists, (1) the used instrumentation and (2) the test environment.

Issue with instrumentation: Authors question the reliability of the available powermeter (Powertap, SRM and G-cog) used in their studies. Authors noted that the instrumentation may have underestimated values [17] or noted a large degree of error [18] [9] [19]. All instrumentation were only capable of collecting overall torque data due to their design, making them unsuitable for a more in-depth analysis of pedal performance. For example investigating left and right leg contribution and the mechanical effectiveness of a pedal stroke.

Issue with environment: Some studies have conducted trials in an environment not considered regulation BMX SX. Laboratory studies of semi-field based studies conducted on a flat ground may have limited transferability to the BMX SX start hill [20] [10] [21]. Therefore, authors advocate for a more field-based approach by running trial under ecological valid conditions².

Up till now instrumentation that meet the sport specific requirements of BMX was lacking. The availability of a wireless instrumented crank capable of collecting radial force and torque data, with 100Hz sample frequency, of left and right leg independently allow pedal force analysis of BMX cyclists under ecological conditions for the first time. The aim of this project was to develop an instrumented BMX bicycle for the members of the Dutch National BMX

²Ecological validity is defined as to what degree results from performed experiments apply, or be generalized, to the real world (i.e. outside the test setting), its a type of external validity. A study can be valid (meet internal and external validity) and not meet ecological validity

team that would allow them to collect objective data on pedalling performance of the gate start and use this for monitoring, bench marking and feedback during training. With the instrumented BMX bicycle this study investigated the research goals; (1) provide a better understanding of how a cyclists effectively propel the bicycle during a BMX gate start, and (2) identify pedalling variables which are good predictors of a fast gate start.

1.5 Thesis structure

Firstly, this thesis report provides background on BMX cycling, reviews the importance of the gate start and previous research regarding pedalling performance in BMX racing in Chapter 1. Furthermore, it presents the motivations and research goals of this work. Thereafter, Chapter 2 contains the environmental setting of the measurements, presents the instrumented cranks and other used materials and describes the measurement procedure, data processing and statistical analyses. Chapter 3 states the definitions of the used performance variables. The results from field-based testing for members of the Dutch track cycling team are presented in Chapter 4. Observational data on movement phases, pedal forces, propulsion and pedalling variables are all presented there. Chapter 5 presents the major findings of this work, and discusses the importance and validity of the results and a comparison with other literature. Finally, conclusions, practical applications and recommendations for future work can be found in Chapter 6

Chapter 2

Methods and materials

2.1 Participants

For this study experimental data were collected on five BMX cyclists (male N=3, female N=2), all members of the Dutch National Team. All cyclists had competed internationally for at least 5 years, were ranked by the Union Cycliste Internationale (UCI) and were a minimum of 18 years of age. Descriptive participant data are provided in Table 2.1. Participants were provided with an information leaflet in advance regarding the aims and procedure of the study. All participants gave their written consent to participate. All study procedures and instrumentation were approved by the Human Research Ethics Committee (HREC) of the TU Delft. Participants wore normal competition clothing, protective gear and standard cycling shoes with clipless pedals. In order to ensure there were no outside influences of other riders, data of one participant was collected during one gate start training session of the team. Data on all participants were collected within a time frame of six weeks.

	age [y]	body mass* (m_b) [kg]	system mass** (m_s) [kg]
mean \pm sd	22 \pm 3	81 \pm 8	91 \pm 8
range	18 - 25	70 - 93	79 - 103

Table 2.1: Descriptive data of participants (male N=3, female N=2). *Body mass is defined as mass rider including competition clothing and protective gear. **System mass is defined as mass of the instrumented bicycle and rider including competition clothing and protective gear.

2.2 Environment

This study was conducted on an 8m high supercross ramp of a regulation BMX course (Arnhem, Netherlands) (Figure 2.1, Table 2.2) equipped with an Olympic standard mechanical start gate (Straight-8, Pro-Gate, Cherry Valley, USA) and random start gate timing sequence (UCI regulations ANNEX 3, document version 01.02.2018) used in international competition.

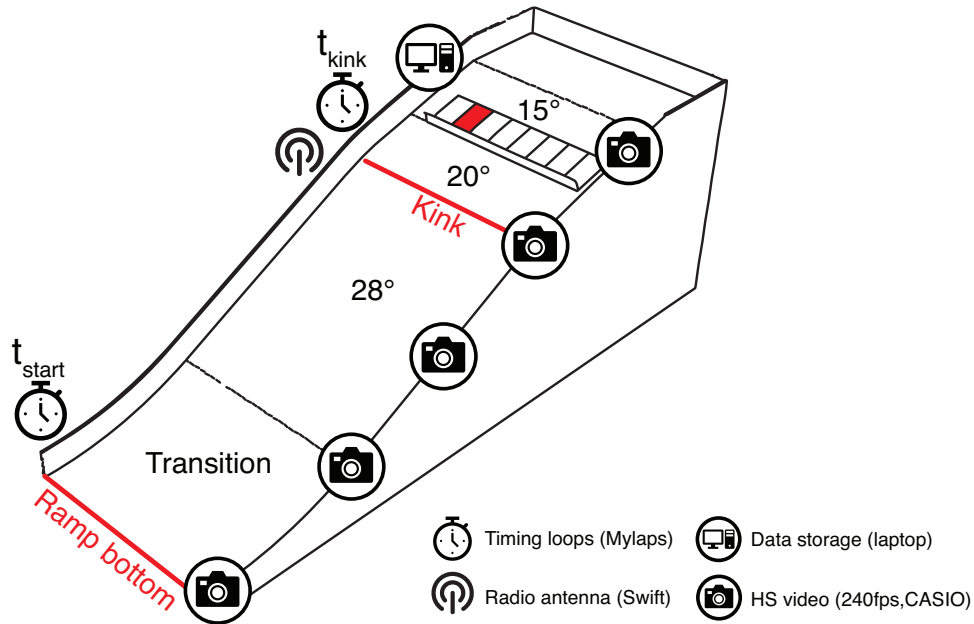


Figure 2.1: Diagram of BMX supercross ramp with experimental setup. Cyclist performed gate start from lane 7 (red box). Ramp slope indication on sections.

Section	Length [m]	Interval [m]	Slope angle* [°]	Comment
Start Gate	1.40	0 - 1.40	15.2	Metal section up to wood
Before Kink	4.43	1.40 - 5.83	20.8	Up to start of kink bend
After Kink	12.50	5.83 - 18.33	28.1	Up to begin of transition
Transition	3.85	18.33 - 22.18	-	Up to wood end bar
Flat	1.79	22.18 - 23.97	0	Up to drainage

Table 2.2: Dimensions of the BMX supercross start ramp (Arnhem, Papendal) used for experiments. *Ramp slope was measured with a digital angle gauge (DAG001, CMT tools, Chiusa di Ginestreto, Italy)

2.3 Experimental set-up

Instrumented BMX bicycle: The instrumented BMX bicycle (Holeshot, Meybo, Boxmeer, Netherlands) (Figure 2.2) was fitted with a set of wireless pre-calibrated instrumented cranks (Axis2D, Swift Performance, Brisbane, AUS; crank length 175mm) (Figure 2.3) to acquire radial force (range $\pm 2500N$) and torque (range $\pm 500Nm$) acting on the crank (sample frequency 100Hz), as well as crank angular velocity (sample frequency 100Hz). The same instrumented crank set was used to test all participants. See Appendix A for a detailed description of the system and data collection. Two custom wheel velocity sensors (see Appendix B for a detailed description) were fitted on the front and rear wheel axle to acquire the angular velocity (200Hz, range $\pm 4000^\circ/s$). On the seat tube of the BMX bicycle frame one 9DoF IMU unit

(Shimmer3, Shimmer, Dublin, Ireland) was fitted to collect acceleration and rotational data of the bicycle frame during the start (400Hz, range $\pm 8g$, $\pm 2000^\circ/s$). IMU data was not analysed in this study.



Figure 2.2: The instrumented BMX bicycle (Holeshoot, Meyboy, Boxmeer, Netherlands) equipped with multiple sensors. Additionally white tapes on the rear rim every 90° make rear wheel rotation better visible on the video recordings.

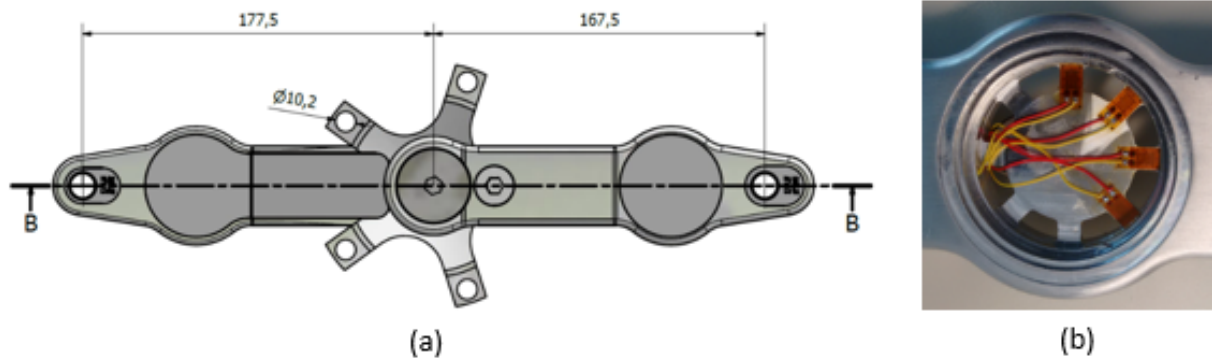


Figure 2.3: Schematic drawing (a) of the Axis2 (Swift Performance, Brisbane, AUS) crank force measurement system, (b) mechanical design and strain gauge configuration for measuring radial and tangential crank force.

Timing: A MYLAPS ProChip (Mylaps Sports Timing, Netherlands) timing system was used to collect the time split (t_{kink}) at the kink and starting time (t_{start}) at the bottom of the ramp, see Figure 2.1. Permanently fixed decoder loops on the ramp detect the passage of two chips (ProChip FLEX, Mylaps Sports Timing, Netherlands) on the BMX bicycle. One attached to the front fork near the front wheel axle and one attached to the chainstay of the frame near the rear wheel axle. Split and ramp time were displayed at a screen on the start ramp and noted after every trial.

Video: Five high-speed cameras (240fps, CASIO Exilim) were fixed to the ramp structure and positioned to provide a sagittal view of the cyclist and the cycling path during the entire gate start, see figure 2.1. Video data was used to calculate the time of the five movement phases defined by Kalichová et al. [6] as in table 2.3. Video data was also used for reference during analyses and synchronisation of timing data with force and velocity data. The first camera was positioned such that the the midpoint of the gate was in the middle of the camera field of view. This resulted in the cyclist starting position being on the right half of the camera view and the start signal lights is visible in the left side of the camera field of view. The second camera was positioned such that the the midpoint of the kink and the start signal light was in the middle of the camera field of view. Two cameras were positioned between the kink and the bottom of the ramp. The last camera was positioned at the bottom of the ramp such that the the midpoint of the timing detection loop was in the middle of the camera field of view. White tape markers were placed on the front and rear wheel axle on the left hand side of the instrumented BMX bicycle to enhance visibility on the video images. In addition four markers were placed on the rear wheel rim with 90° interval to enhance visibility of rear wheel rotation on the video images. One recording file per trial per camera was made, locally stored with a time stamp, on a micro SD card for post processing.

Phase	Definition
1. Reaction time	From the time of the red start light ($t = 0$ s) till moment of movement initiation.
2. Preparation movements	Starts moment of movement initiation and finishes at the initiation of the first pedal stroke.
3. First pedal stroke	From at initiation of first pedal stroke till the cranks are parallel with direction of gravity, i.e. vertical.
4. Dead point pedal passage	Time delay between first and second pedal stroke.
5. Second pedal stroke	From initiation of second pedal stroke till cranks are vertical again.

Table 2.3: The BMX gate start divided into five phases as defined by Kalichová et al. [6]

2.4 Procedure



Experiments were conducted during regular gate start practice sessions of the team. The participant used an instrumented BMX bicycle in their own size and personal handlebar, making it identical to their personal bicycle, a Meybo Holeshot model. Due to limited availability of BMX chain rings which fit the instrumented crank the gear ratio was fixed (44/16). Rear wheel tire was chosen (20" x 1.75 or 20" x 1.60) to meet preferred gear ratio. The wheel circumference was determined by measuring the distance covered with one full rotation of the rear wheel with the participant on the bike. Participant body mass (m_b) with shoes and helmet, and combined mass of bike and rider (system mass, m_s) was measured with a scale (SECA 803, Seca group, Germany). Prior to the experiments, the participant completed a self-selected, typical warm-up routine on the instrumented bicycle to get familiar with the instrumented bicycle.

After the warm-up a zero offset data file was made from the instrumented cranks; Cranks were placed in vertical position with the left crank in the Top Dead Center (TDC), a digital angle gauge (DAG001, CMT tools, Chiusa di Ginestreto, Italy) was used to verify the vertical position before the crank angle was set to zero in the provided Graphical User Interface (GUI) of the crank set. Thereafter a zero offset file of 10 seconds was recorded in order to determine the zero offset values for radial force and torque during post processing of the data (calculate the mean value over 10 seconds of the zero offset file and deduct on trial data).

Participants performed six individual maximum effort start trials on the supercross start ramp (Arnhem, Netherlands), only the participant lined up for each start. For practical reasons all participants used start lane 7 for all trials (see red area in Figure 2.1); This position was experimentally determined to be least admissible for crank data package loss when the gate was up, since data could only be recorded after wireless transmission. Participants were instructed to perform the trials as fast as possible until the first jump. Initial crank angle was self-selected. Split time and ramp time were noted from the timing data logging program.

Upon return the participant first rate their performance subjectively on a Visual Analogue Scale [22] [23] [24] (Figure 2.4) before knowing their split and ramp time. Recovery time between starts was self-selected with a minimum of 5 minutes in length to maintain maximal short sprint abilities [25].

Trial #: How good was this start? Mark the line below.

Very bad  |-----|  Very good

Comment:

Figure 2.4: Visual Analogue Scale (VAS), a non-specific measuring scale, for one trial. The horizontal line is 100 mm, minimum score is on the left and the maximum score is on the right. Participants rate their trial by drawing a vertical line along the horizontal line, the distance between the participant vertical line and the minimum score is the score on the VAS [22] [23] [24]. Participant could leave a specific comment on their performance in addition to the VAS score if they wished to do so.

For video, wheel velocity and crank force data individual data log file's with time stamp were created for every trial to facilitate post processing. IMU data was continuously recorded during the entire duration of one experiment and stored in one data file.

2.5 Data processing

Calibrated crank data was stored on two separate CSV files for left and right crank data and exported for further analysis with numerical computing environment MatLab (version R2019a, The MathWorks, Inc., Natick, USA). In Matlab synchronisation and manipulation of the data was performed before detailed analysis. Left and right crank data was synchronised by performing a cross correlation on the crank angle data. From the zero offset file the zero offset is determined, radial force and torque data is corrected by subtracting the zero offset value. Trial data was synchronised based on the onset of definitive forward crank rotation (i.e. definitive forward bike velocity). Forward propulsion was defined as the positive crank rotation and positive torque direction, positive radial force was defined as elongation of the crank arms. Torque and force measurement are filtered using a Savitzky-Golay filter [26] with span 0.04 and degree of 2, crank angle velocity was smooth with a robust local regression [27] with a 0.05 span using weighted linear least squares and a 2nd degree polynomial model.

Video Video data was processed using Kinovea, a free and open source video player for sports analysis (Kinovea version 0.8.15, kinovea.org, France). Video files are cropped, the illumination of the red light on the start signal was considered as the beginning of a trial. The

onset of the green light, the gate drop and the interval times of the five movement phases were manually determined noting the corresponding frame number. The time between the the red light and initiation of forward velocity of the rear wheel (i.e. initiation of first pedal stroke) was used to time synchronise the crank and wheel velocity sensors data with the timing data.

2.6 Statistical analysis

Firstly, to decide how strength related variables could be best scaled, correlations to t_{start} were compared for absolute, ratio scaled (to body mass) and allometrically scaled (to body mass^{2/3})[28] [29], presented in table 2.4. Pearson correlations were all significant ($p < 0.01$) except for ratio scaled L2_Fr_max and T1_P_max. Based on Fisher r-to-z transformation correlations of ratio scaled variables were significantly different ($> \pm 1.96$) from absolute values (indicated (#) in the table). Therefore, its decided to perform analyses using both absolute as ratio scaled strength data.

To identify the potential performance variables the Pearson's product-moment correlation was used to investigate the relationship between the potential performance variables and the starting time. The significance of strong correlations over 0.5 and below -0.5 were then determined. Statistical significant was set at $P < 0.05$.

Relative importance of the potential performance variables are then analysed using stepwise linear regression [30] where enter p-value is set to 0.06 and significant threshold at 0.05. The performance of the stepwise linear regression model are judged on adjusted R squared (R_{adj}^2), Shapiro-Wilk normality test [31] and on the standardized normal probability plot. To investigate between- gender differences independent sample t-test were conducted. A one-way ANOVA was conducted to investigate between-participant differences.

Variables	Absolute	Ratio	Allometrically
		/kg	/kg ^{2/3}
W_top	-0.95*	-0.60*#	-0.82*#
W_bottom	-0.83*	-0.70*	-0.77*
Tmax	-0.92*	-0.59*#	-0.81*
Pmax	-0.90*	-0.81*	-0.87*
L1_Fe_max	-0.93*	-0.73*#	-0.88*
T1_Fe_max	-0.88*	-0.56*#	-0.75*
L2_Fe_max	-0.89*	-0.62#	-0.82*
T2_Fe_max	-0.79*	-0.54*	-0.65*
L1_Fr_max	-0.91*	-0.77*	-0.87*
T1_Fr_max	-0.88*	-0.59*#	-0.75*
L2_Fr_max	-0.88*	-0.33#	-0.69*
T2_Fr_max	-0.83*	-0.66*	-0.74*
L1_P_max	-0.91*	-0.88*	-0.90*
T1_P_max	-0.80*	-0.32#	-0.54*
L2_P_max	-0.87*	-0.67*	-0.82*
T2_P_max	-0.85*	-0.67*	-0.76*

Table 2.4: Pearson correlations for strength related variables. *strong correlation with t_{start} . # significant difference with respect to absolute correlation based on Fisher r-to-z transformation.

Chapter 3

Definitions of performance variables

3.1 Dependent variable

3.1.1 Starting time (t_{start})

Starting time [s] is recorded by a timing system (Mylaps Sports Timing, Netherlands) and is defined as the time interval between the illumination of the green start signal light and the passage of the front wheel over the decoder loop at the bottom of the start hill. More specifically the passage of the timing chip (ProChip FLEX, Mylaps Sports Timing, Netherlands) attached to the front fork of the bicycle near the wheel hub.

3.2 General performance variables

3.2.1 Velocity at gate drop (V_i)

Velocity of the BMX bicycle at the moment the gate starts to drop. Crank angle velocity is calculated from crank angular position signal:

$$\omega_i = (\theta_i - \theta_{i-1}) \cdot f_s \cdot \frac{\pi}{180} \quad (3.1)$$

Where ω_i is the crank angular velocity in [rad/s] for data point i , θ is the crank angle in [$^\circ$] and f_s is the sampling frequency of the signal in [Hz]. The rear wheel ground velocity is calculated from the crank angle velocity by:

$$V_{bike_i} = \omega_i \cdot GR \cdot \frac{C}{2 \cdot \pi} \quad (3.2)$$

Where V_{bike_i} is the rear wheel ground velocity in [m/s] for data point i , GR the gear ratio and C the rear wheel circumference. Using video analyses the time interval (t_{gate}) between initiation of forward velocity and the moment the gate starts to drop is determined to find the initial velocity at the gate drop:

$$V_i = V_{bike_{t_{gate}}} \quad (3.3)$$

Where $V_{bike_{gate}}$ is the rear wheel ground velocity when the gate drops in [m/s] and is called the initial velocity (V_i) in [m/s].

3.2.2 Mass (m)

Devided into:

- m_b : body mass in [kg], mass of rider with all (protective) gear.
- m_s : system mass in [kg], mass of rider with all (protective) gear and the instrumented bicycle.

3.2.3 Work (W)

To compare between riders the energy production during the start is calculated for every trial. Work done (W) over every data point (i) is:

$$W_i = T_{total_i} \cdot \Delta\theta \quad (3.4)$$

Where T_{total} is the sum of the left and right torque in Nm and $\Delta\theta$ is the crank rotation ($\theta_i - \theta_{i-1}$) in radians. The cumulative sum (S) of the work done tells us on every point in during the start how much work the rider has put in up till then:

$$S_k = \sum_{i=1}^k W_i \quad (3.5)$$

The average work done (\bar{W}) over 20cm traveled distance intervals (x) ($dx = 0.2m$) becomes:

$$\bar{W}_j = \int_{x_j}^{x_{j+dx}} \bar{S} dx \quad (3.6)$$

where \bar{S} is the average of the cumulative work values within the 20cm distance interval.

3.2.4 Torque peak (T_{max})

Maximal value over a trial from the sum of the left and right torque crank data after filtering.

3.2.5 Power peak (P_{max})

Maximum value over a trial from the continues power. Where continues power is:

$$T_{net} = T_{left} + T_{right} \quad (3.7)$$

$$P = T_{net} \cdot \omega \quad (3.8)$$

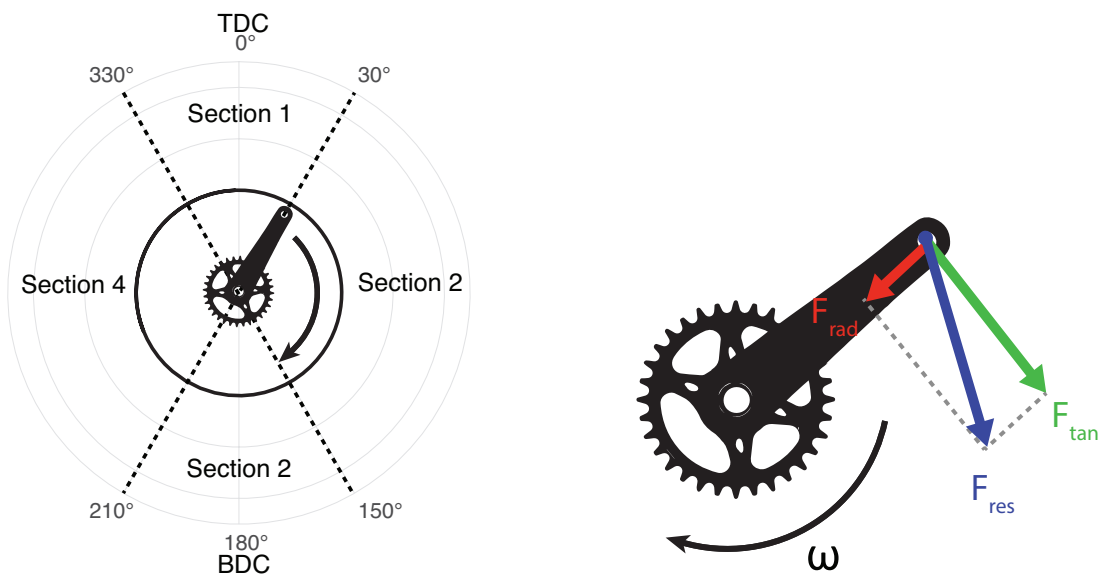
Where T_{left} and T_{right} is the torque from the left and right crank respectively in [Nm], ω_i is the crank angular velocity in [rad/s].

3.2.6 Time to power and torque peak ($t-T_{max}$, $t-P_{max}$)

Time when continues power peak and torque peak is reach where $t = 0$ is the moment of initiation of forward velocity.

3.3 Pedal performance variables

The crank revolution can be divided into four section, as shown in Figure 3.1. Section 1 is the area around top dead center (TDC at 0° crank angle), section 2 is the push phase of the pedal stroke, section 3 is the areas around the bottom dead center (BDC at 180° crank angle) and lastly section 4 which is the pull phase of the pedal stroke.



(a) Sections of the pedal stroke. section 1 is the TDC area, section 2 the push phase, section 3 the BTC area and section 4 the pull phase

(b) Applied force on the pedal, i.e. Resultant force (F_{res} , blue arrow), divided in effective force, i.e. crank tangential force (F_{tan} , green arrow), and unused force, i.e. crank radial force (F_{rad} , red arrow). Crank rotates with crank angular velocity (ω)

Figure 3.1: Visualisation of (a) crank revolution sections and (b) pedal forces

3.3.1 Effective force peak (Fe_{max})

Effective force is the force in the tangential direction of the crank arm calculated by:

$$Fe = T/CL \quad (3.9)$$

Where T is the torque recording [Nm] and CL is the length of the crank arm [m]. Fe_{max} is

defined as the maximum tangential force of one leg during a pedal stroke.

3.3.2 Resultant force peak ($F_{r_{max}}$)

Resultant force is the applied force on one pedal and is the sum of the tangential and radial crank force as in:

$$F_{res} = \sqrt{F_{tan}^2 + F_{rad}^2} \quad (3.10)$$

Where F_{tan} is the tangential crank force [N] and F_{rad} the radial crank force.

3.3.3 Power peak per pedal stroke

Maximum power value [W] over a pedal stroke.

3.3.4 Relative Maximum Power Duration ($RMPD_{90}, RMPD_{70}$)

The Relative Maximal Power Duration ($RMPD$ [°]) introduced by Bertucci et al. [13] quantifies a cyclist ability to produce instantaneous power above 90% ($RMPD_{90}$) or 70% ($RMPD_{70}$) of the P_{max} over a large crank angle interval. $RMPD$ was defined as the crank angle interval during which the instantaneous power remained higher than 90% and 70% of the P_{max} respectively.

3.3.5 Index of force Effectiveness (IE)

Pedal force effectiveness and can be quantified by the Index of Effectiveness (IE) [2]. This mechanical effectiveness is defined as the ratio of the impulse of the tangential crank force (i.e. the effective force) to the impulse of the total force applied to the pedal (i.e. the resultant force) over one crank revolution as in:

$$IE = \frac{\int_{30^\circ}^{210^\circ} F_{tan} \cdot dt}{\int_{30^\circ}^{210^\circ} F_{res} \cdot dt} \quad (3.11)$$

Since IE is highly dependent on the push phase of the pedal stroke [32] and to make it independent from the Push Pull ratio, IE is calculated over section 2 and 3 of the crank cycle, i.e. from 30° till 210° .

3.3.6 Push Pull ratio (PP)

The Push Pull ratio (PP) provides information and the contribution of pulling on the pedal during the upstroke of the crank cycle to the total torque production. PP is defined as the ratio of the impulse of the pulling force to the impulse of the total force over a crank cycle as in:

$$PP = \frac{\int_{210^\circ}^{30^\circ} \text{pull leg } Fe \cdot dt}{\int_{30^\circ}^{210^\circ} \text{push leg } Fe \cdot dt} \quad (3.12)$$

Where the angles are with respect to the mentioned leg, i.e. its the ratio of the effective force of the pull leg over section 4 and 1 to the effective force of the push leg in section 2 and 3 within one crank cycle.

3.3.7 Dead center size (DC)

Dead Center size (DC) provides information on a cyclists ability to overcome a crank position where it is seemingly very difficult to produce high power output; at the top and bottom of the crank cycle, Top Dead Center (TDC) and Bottom Dead Center (BDC) respectively. DC is defined as the pedal work rate in these difficult sections compared to the average work rate through a crank cycle. For a crank cycle this is calculated as:

$$DC = \frac{\bar{P}_{section1} + \bar{P}_{section3}}{\bar{P}_{crank}} \quad (3.13)$$

Chapter 4

Results

Start times, velocity and crank based data from 27 starts (5 participants) were available for analysis. For two trial the left crank data was missing and for one trial the gate video (needed to determine the velocity at the gate drop) was missing due to practical issues.

4.1 Movement phases

The following table presents the interval times of the five individual start phases. Table 4.1 presents results over all trials of every rider and table 4.2 presents the the grouped results for all, male and female riders.

Phase	Time [s] (Mean \pm Std)				
	Rider 1 (σ)	Rider 2* (σ)	Rider 3* (σ)	Rider 4 (φ)	Rider 5 (φ)
1. Reaction [†]	0.180 \pm 0.019	0.188 \pm 0.025	0.156 \pm 0.011	0.177 \pm 0.010	0.190 \pm 0.011
2. Preparation [‡]	0.203 \pm 0.012	0.213 \pm 0.023	0.240 \pm 0.008	0.250 \pm 0.021	0.267 \pm 0.022
3. 1 st pedal stroke [‡]	0.400 \pm 0.015	0.419 \pm 0.017	0.424 \pm 0.004	0.392 \pm 0.010	0.313 \pm 0.009
4. Dead center [†]	0.063 \pm 0.007	0.071 \pm 0.011	0.059 \pm 0.015	0.057 \pm 0.005	0.078 \pm 0.011
5. 2 th pedal stroke [‡]	0.342 \pm 0.012	0.350 \pm 0.013	0.330 \pm 0.019	0.365 \pm 0.015	0.408 \pm 0.015
Sum [‡]	1.197 \pm 0.020	1.240 \pm 0.019	1.209 \pm 0.008	1.242 \pm 0.018	1.255 \pm 0.018

Table 4.1: Individual interval time per movement phase of the BMX start as defined by Kalichová et al. [6], see also table 2.3 for phases description. [†] significant between-participant difference ($P < 0.01$). [‡] significant between-participant difference ($P < 0.001$). Male (σ): rider 1,2 and 3. Female (φ): rider 4 and 5). Riders used a gear ratio of 44/16 in combination with a rear wheel circumference of 1.535 m (20"x1.60 tire), *different rear wheel circumference: 1.587 m (20"x1.75 tire).

Phase	Time [s] (Mean \pm Std)		
	All riders	Male (σ)	Female (φ)
1. Reaction	0.178 \pm 0.012	0.175 \pm 0.013	0.183 \pm 0.006
2. Preparation	0.234 \pm 0.024	0.218 \pm 0.016	0.259 \pm 0.016
3. 1 st pedal stroke	0.390 \pm 0.040	0.414 \pm 0.010[‡]	0.352 \pm 0.039[‡]
4. Dead center	0.066 \pm 0.008	0.064 \pm 0.005	0.067 \pm 0.006
5. 2 th pedal stroke	0.359 \pm 0.027	0.341 \pm 0.008	0.387 \pm 0.025
Total	1.229 \pm 0.022	1.215 \pm 0.018	1.248 \pm 0.013

Table 4.2: Grouped interval time per movement phase of the BMX start as defined by Kalichová et al. [6], see also table 2.3 for phases description. ‡ significant between-gender difference ($P < 0.001$). Male (σ): rider 1,2 and 3. Female (φ): rider 4 and 5).

The total phase time ranged between 1.158 – 1.267 seconds and 1.217 – 1.296 seconds for male and female respectively. The longest phase was phase 3 (i.e the first pedal stroke) for male riders and phase 5 (i.e. the second pedal stroke) for female riders. For male riders the second pedal stroke took 17.6% less time compared to the first pedal stroke, where for female riders the second pedal stroke was 9.9% slower compared to their first pedal stroke.

4.2 Crank data

The calibrated data from both instrumented crank arms were stored as CSV file using the manufacturer software. After importing the data in MatLab (version R2019a, The MathWorks, Inc., Natick, USA), Figure 4.1 shows an example recording from the left and right crank during a gate start. The torque, radial force and angular position of both cranks where recorded and shown in the top, middle and bottom plot respectively. The area's highlighted with red dashed line indicate issues that need to be addressed. When the torque exceeds 325.8Nm there appears to be a sign flip and the value becomes negative, shown in area A. Area B in highlight the issue of missed packages due to the wireless data transmission before storage. There is a slight time shift between the left and right crank data, highlighted in area C.

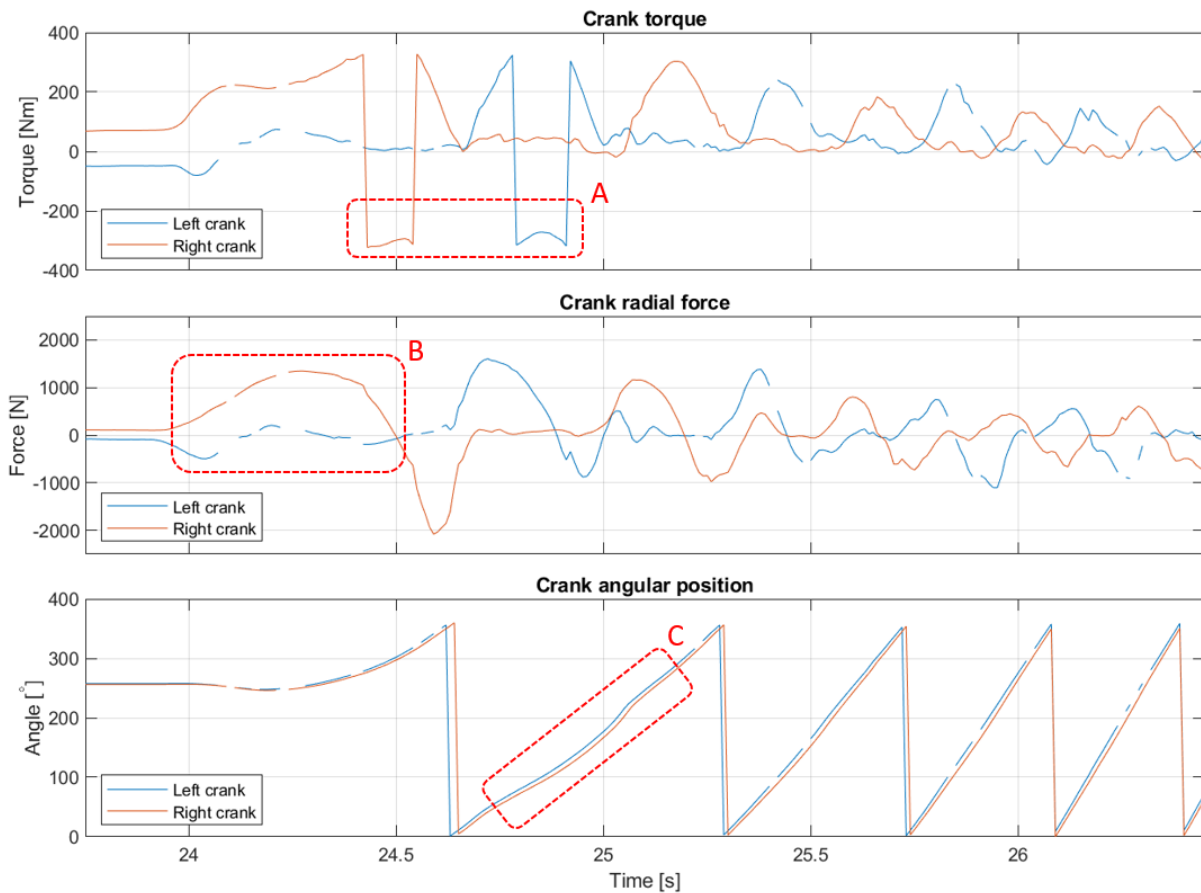


Figure 4.1: Example recording from instrumented Axis2D cranks from Swift Performance on one gate start. Calibrated crank data from left and right crank. Torque, radial force and angular position is shown in the top, middle and bottom plot respectively. Area's within red dashed lines highlights data issues; A) incorrect negative value for torque data when exceeding $325.8Nm$, B) data gaps due to missed packages in wireless transmission and C) time shift between left and right crank data.

The incorrect negative torque values were identified and corrected to positive values. Since the duration of lost data point is short a linear interpolation provides an approximation for the missing data. Synchronization of left and right crank data was done by means of a cross-correlation on the angle position of both cranks. The zero offset values taken from the 10 second zero offset file that was recorded at the beginning of each experiment were subtracted from the torque and radial force data. Furthermore, for convenience, the radial force data was multiplied by -1 so that positive sign would represent extension of the crank arm. After application of these adjustments the data file of the example recording is shown in Figure 4.2 and used for further analysis.

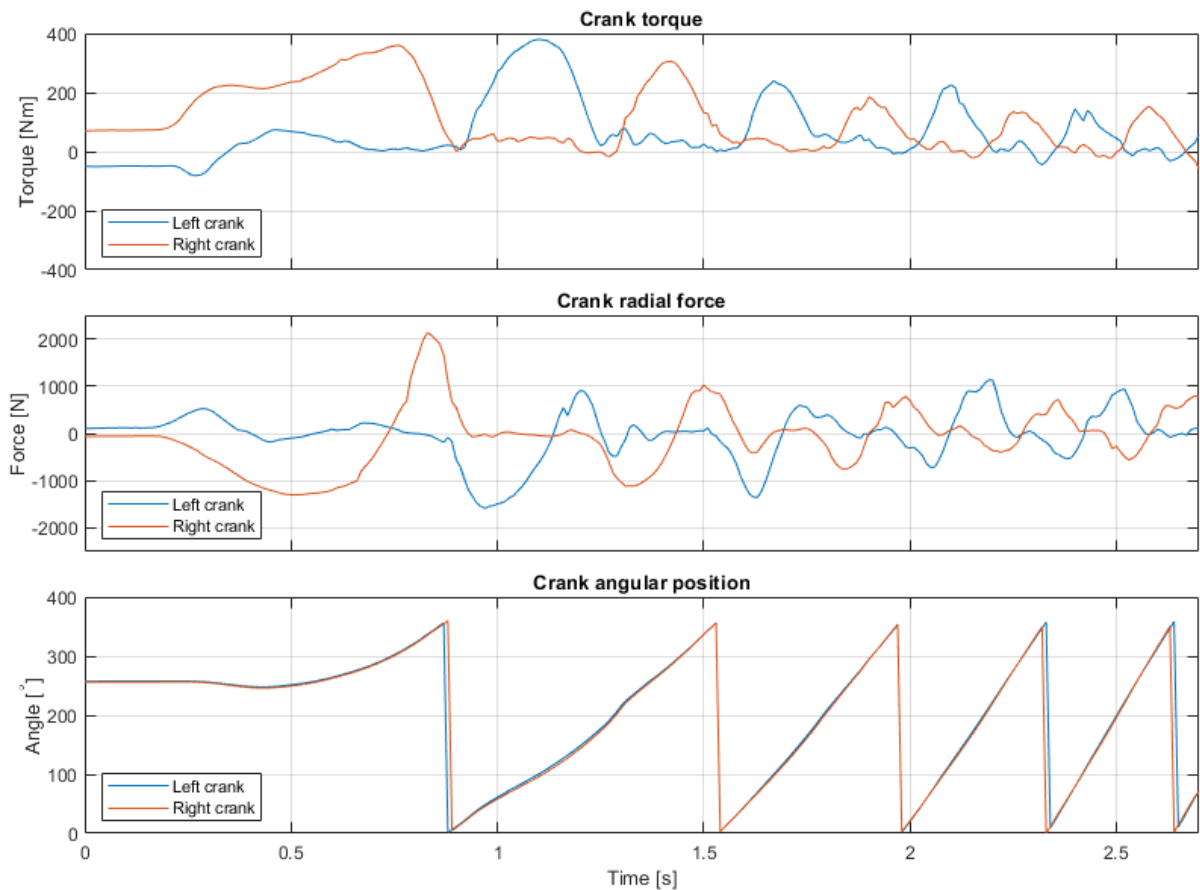


Figure 4.2: Example recording from instrumented Axis2D cranks from Swift Performance on one gate start after corrections done in Matlab (version R2019a, The MathWorks, Inc., Natick, USA). Calibrated crank data from left and right crank. Torque, radial force and angular position is shown in the top, middle and bottom plot respectively. Positive torque is in the direction of effective torque. Positive radial force is in the direction of elongation of the crank arm. Left crank data in blue, right crank data in orange.

4.3 Propulsion

4.3.1 Pedal forces

An example of the pedal forces of the first two pedal strokes are given in Figure 4.3. At the moment of initiation of forward velocity the crank angle position is around 65° . Effective force peak is reached in the push phase of the pedal stroke. The effective force barely drops below 0N during the first two pedal strokes, especially during the pull phase of the crank revolution both legs still have a positive contribution to propulsion. Resultant force peak is reached on the boundary between the push phase and the BTC section.

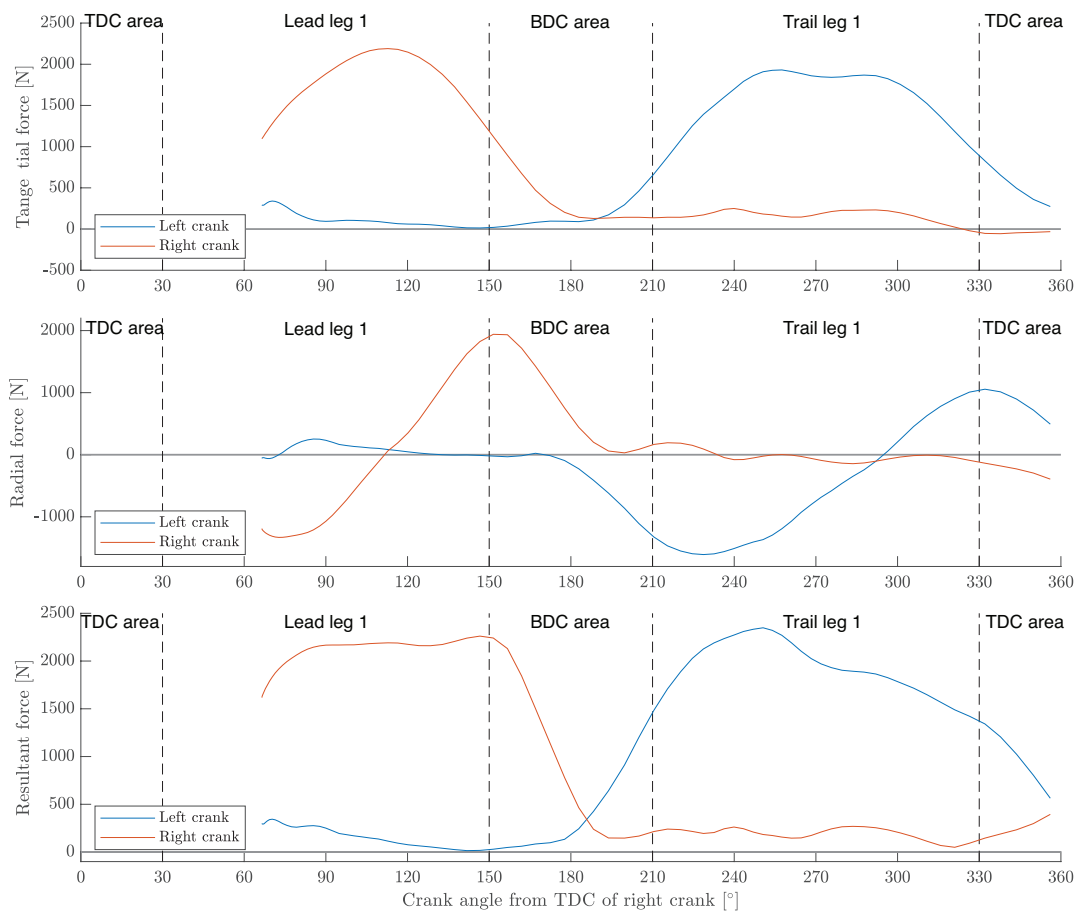


Figure 4.3: Example recording of pedal forces of the first and second pedal stroke. The graph shows the force from the moment of initiation of forward velocity. Tangential force is calculated from the torque signal, Resultant force is the combination of tangential force and radial force and represents the force applied on the pedal. The crank angle of the right crank is given on the x-axis.

4.3.2 Torque-cadence profile

Figure 4.4 shows the torque-cadence graph of the pedal forces in Figure 4.3. The torque is the total propulsive torque from the left and right crank combined. From the crank angle recording the crank angle velocity (in deg/s) was derived and converted to an equivalent cadence ($/min$).

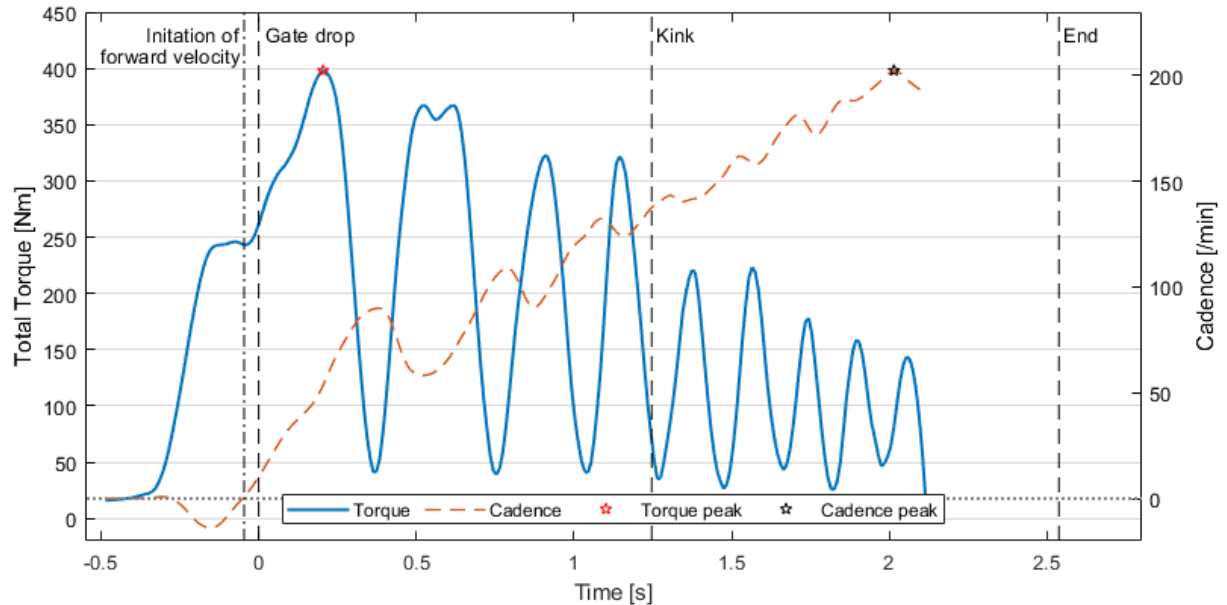


Figure 4.4: Example of a gate start trial. Torque and crank angular velocity both measured with Axis2D instrumented cranks (Swift performance). Both signals recorded at 100Hz. Total torque is the combination of left and right crank effective torque measurement.

The initiation of forward velocity (black vertical dashed-dotted line) generally takes place before the gate drop (black vertical dashed line). Before the initiation of forward velocity the torque is held constant. Torque peak generally is reached on the first pedal stroke, indicated by the red star. The first four pedal stroke distinguish themselves from the later pedal stroke by their higher torque peaks. The fourth pedal stroke generally takes place when the rear wheel is located on the kink. In the second pedal stroke a small dip in torque can be seen during the peak torque, the video recording shows a movement imbalance during that time frame for this example trial. Short after the cadences peak (black star) is reached the data stream ends, indicating the rider stopped pedalling. The bottom of the start hill reached at the dashed line indicated with 'End', this is the location of the timing decoder loop and therefore the dashed line indicated the start time of the example trial.

4.3.3 Power-velocity profile

Figure 4.5 shows the power and velocity profile of the same trial as the previous two figures. The blue line represents continues power data calculated from total torque and crank angular

velocity data. The black horizontal line represent mean power over the concerned pedal stroke (over 0° - 180° or 0° - 180° crank angle). The dashed orange line presents the rear wheel velocity recorded with the custom speed sensor. At the end of the trial, right after the the rider stops pedalling there is a sudden increase in velocity followed by a sudden constant velocity before the velocity drops slightly at the end of the start hill. This happens on the transition zone of the starting hill where riders prepare for the first jump.

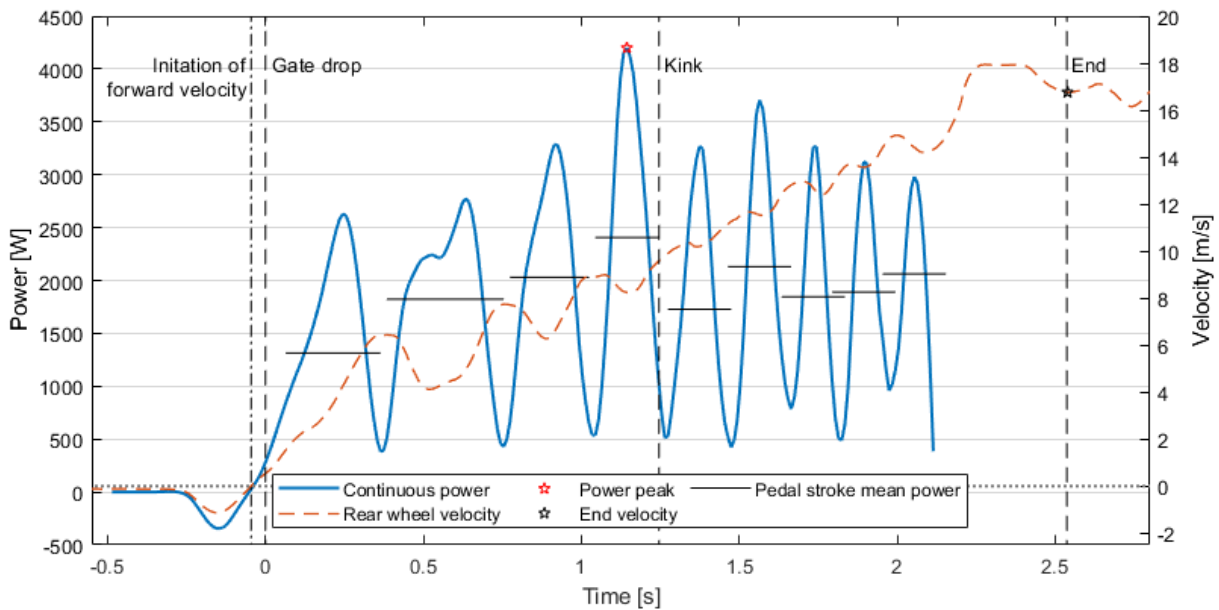


Figure 4.5: Example of a gate start trial. Power and rear wheel velocity. Power calculated from total torque and crank angular velocity both recorded at 100Hz. Rear wheel velocity was recorded at 200Hz with custom speed sensor.

4.4 Work

For rider 1 the result is presented in Figure 4.6, see Appendix C for result of all riders.

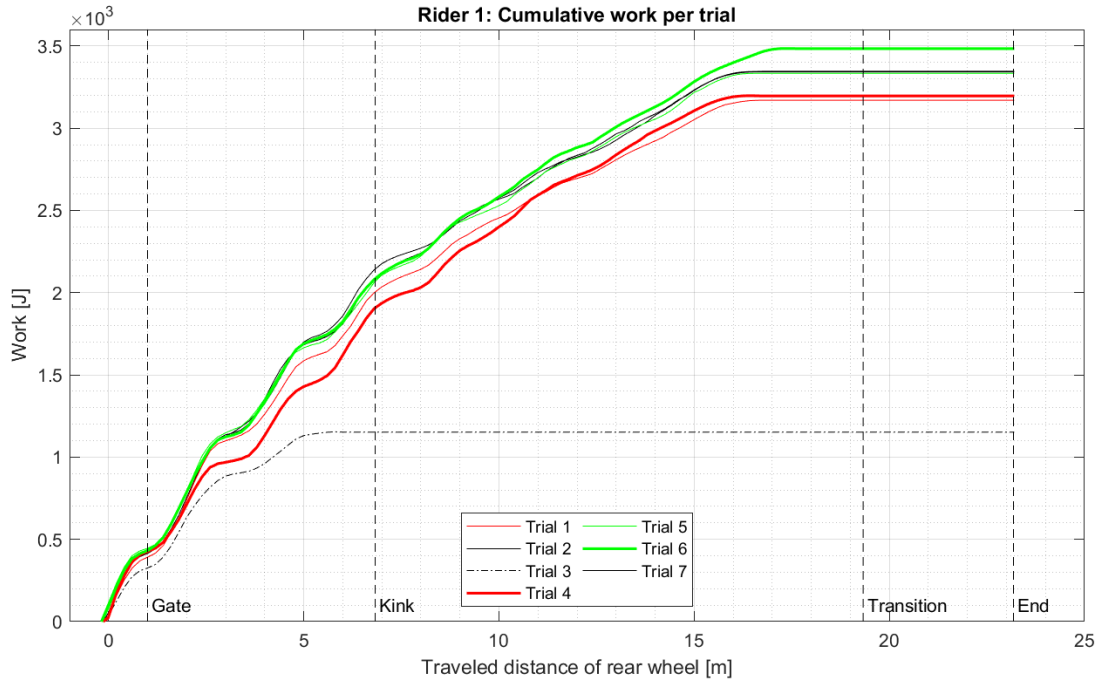


Figure 4.6: Cumulative work done by rider 1 for every trial over the traveled distance on the start ramp. In red (Trial 1 and 4) the two slowest starting times (t_{start}) in which the bold line is the slowest trial (Trial 4), in green (Trial 5 and 6) the two fastest start times in which the bold line is the fastest trial (Trial 6). Trial 3 (black dashed point line) was discontinued prematurely by the rider because of hitting the gate with the front wheel. 0 m is the contact point between the rear wheel and the ramp. The horizontal line at end of the ramp means no added work over that distance, i.e. stopped pedalling at the end of the ramp to prepare for the first jump.

For every rider the mean cumulative work done (W_{mean}) over all trials have been calculated and shown in Figure 4.7.

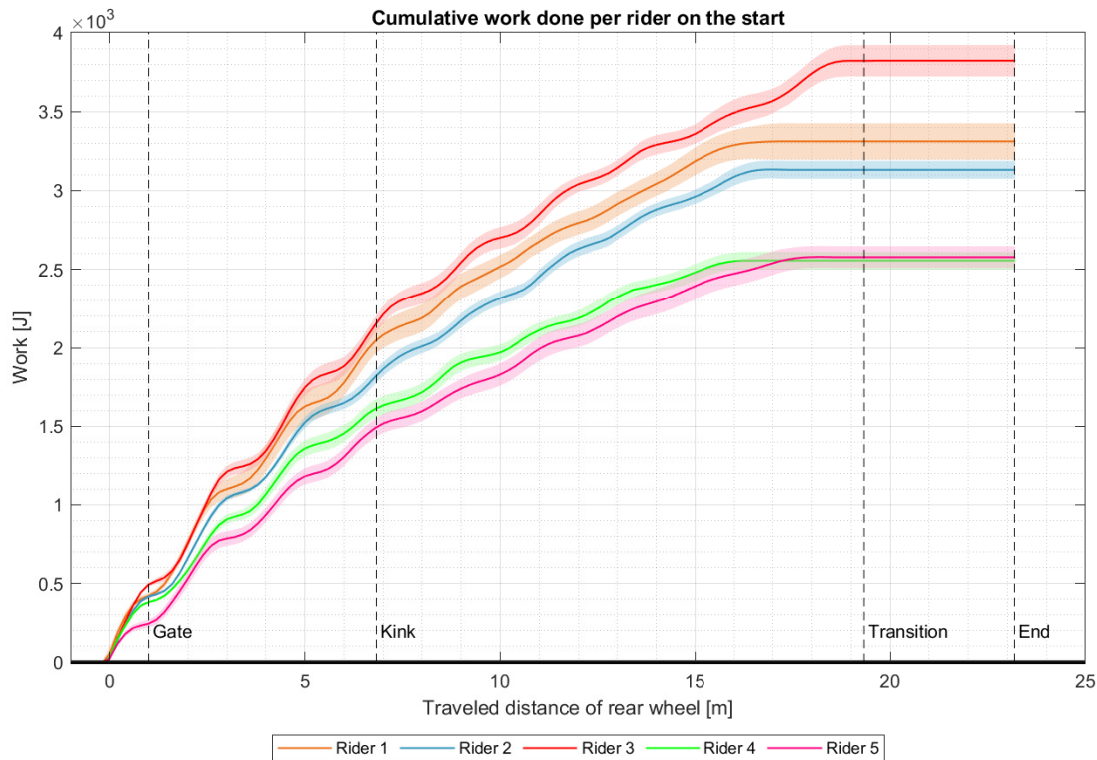


Figure 4.7: Mean cumulative work done per rider. Solid line represents mean work (\bar{W}) in Joule of all trial of a rider, transparency area around solid line represents the standard deviation (STD) from the mean work over all trials. 0 m is the contact point between the rear wheel and the ramp. There is a clear difference between male riders (rider 1, 2 and 3) and female riders (rider 4 and 5). 2003 ± 138 and 1542 ± 86 Joule respectively for work up to the kink ($P < 0.001$), and for work after the kink 1509 ± 254 and 1057 ± 58 Joule respectively ($P < 0.001$)

The graph visualises the differences between riders in where they put in work over the distance of the start ramp. When the gradient of the cumulative work becomes zero at the end of the start, i.e. a horizontal line, indicated the rider has stopped pedalling before the end of the ramp. There is a difference between female riders (rider 4 and 5) compared to the male riders (riders 1,2 and 3). Rider 4 has produced more work up to the kink compared to rider 5 (1616 ± 50 and 1493 ± 68 Joule respectively, $P < 0.05$), but rider 5 is able to generate more work in the latter portion of the start (997 ± 25 and 1098 ± 28 Joule respectively, $P < 0.001$).

The gradient of the cumulative work is larger for the traveled distance up to kink then it is after the kink. Up to 60% of the total work done before the kink, when only 25% of the total distance of the start ramp has been traveled. Table 4.3 provides the distribution of the work for every rider over the sections before and after the kink in the percentage of the total work done over the start.

Participant	0m - Kink [%]	Kink - End [%]
Rider 1	61.7	38.3
Rider 2	57.9	42.1
Rider 3	56.2	43.8
Rider 4	62.9	37.1
Rider 5	57.7	42.3
Mean \pm std	59.3 \pm 2.6	40.7 \pm 2.6

Table 4.3: Work done expressed in the percentage of total work for every rider over the distance before the kink and the distance after the kink.

The total energy input during the start (E_{in}) consists of work and potential energy (E_{pot}):

$$E_{in} = W + E_{pot} \quad (4.1)$$

Where $E_{pot} = m \cdot g \cdot h$, (i.e. mass(m), gravity (g) and height (h)).

With respect to the total energy input the contribution of work done by the rider is shown in Table 4.4.

Participant	Gate - Kink [%]	Kink - End [%]	Gate - End [%]
Rider 1	51.1	17.5	29.6
Rider 2	46.8	17.1	27.2
Rider 3	48.9	19.4	29.4
Rider 4	45.5	13.8	24.7
Rider 5	46.1	16.9	26.7
Mean \pm std	47.7 \pm 2.1	17.0 \pm 1.8	27.5 \pm 1.8

Table 4.4: Work contribution to total energy input during the start in percentage. For the two section (Gate-Kink and Kink-End), and over the complete start hill (Gate-End).

Up to the kink the contribution of work done by the riders are around 50% of the total energy input up to that point. After the kink the contribution of work by pedalling drops drastically to only 17%, the mean energy source for this section is the potential energy. Over the whole duration of the start the contribution of pedalling is around 27% with respect to the total energy input.

4.5 Performance variables

4.5.1 General variables

The relation between the general variables and the starting time is presented in Figure 4.8.

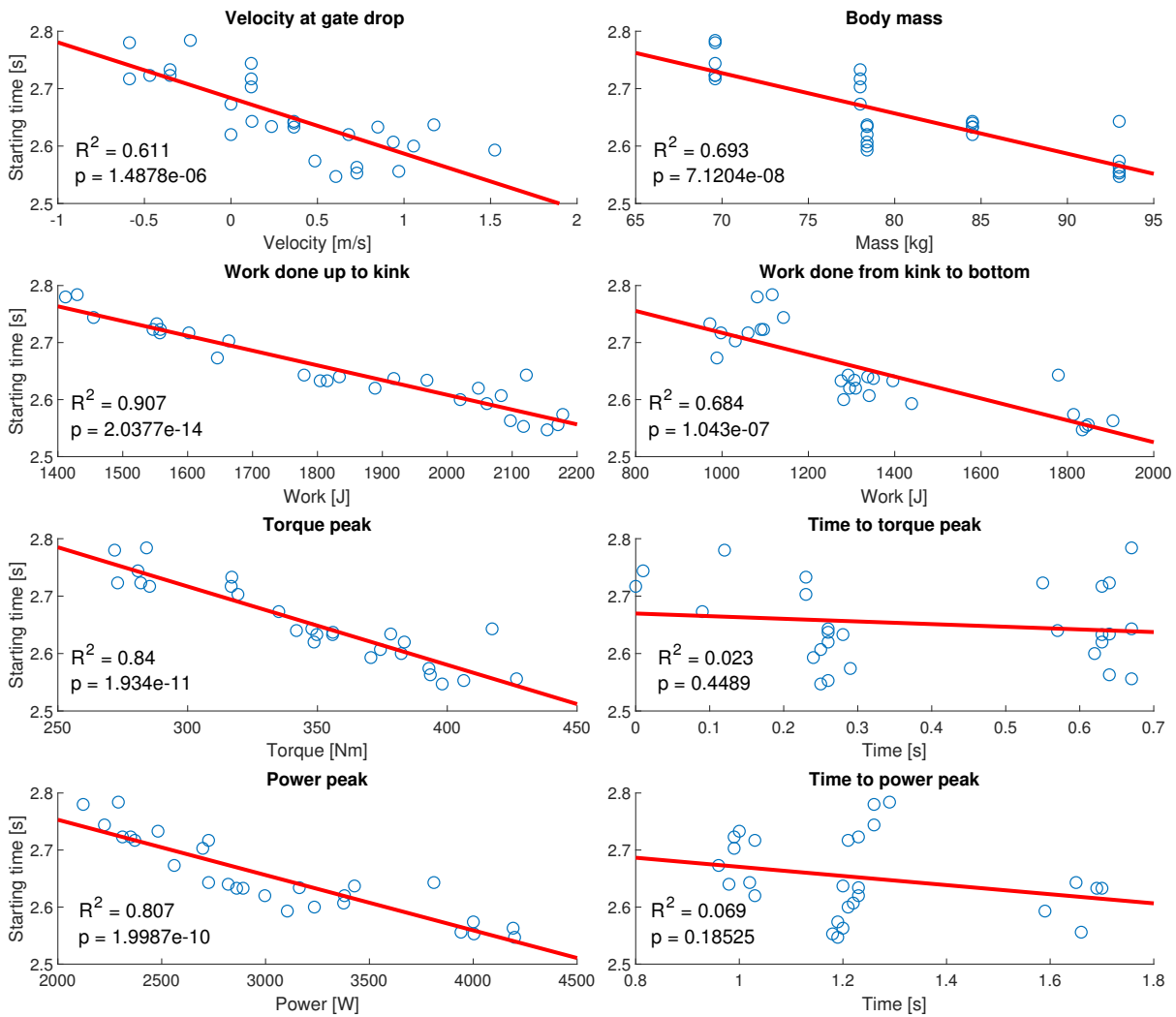


Figure 4.8: Relationship between general variables and starting time

Work done up to the kink explains over 90% (the most of all variables) of the variation in the starting time and has the highest statistical significance. Time to peak torque and time to peak power do not show a significant relation with respect to the starting time. Work done from kink to bottom seems to have 3 clusters of data points. The data point in the cluster on the far right belong to one rider who performed one pedal stroke more then the other riders before preparing for the first jump. The data points in the cluster on the far left belong to the female riders. Time to torque en power peak also seem to have clustered data, not surprisingly considering that maximum peaks can occur in different pedal strokes.

Descriptive data of the general variables is presented in table 4.5 for all trials and for male (n=17) and female (n=10) trials separately. Details of all the regression models are presented

in Appendix D.

General variables			All	Male	Female	range
Starting time	t_{start}	[s]	2.652±0.07	2.606±0.035 [†]	2.73±0.033	2.547-2.784
Velocity at gate drop	V_i	[m/s]	0.33±0.56*	0.66±0.4 [†]	-0.22±0.29*	-0.59-1.52
Work up to kink	W_{top}	[J]	1833±257*	2003±138* [†]	1542±86*	1412-2178
		[J·kg ⁻¹]	22.7±1.9*	23.5±1.8 [†]	21.2±0.9	19.9-26.6
Work after kink	W_{bottom}	[J]	1342±301*	1509±254* [†]	1057±58*	972-1906
		[J·kg ⁻¹]	16.5±2.3*	17.6±1.8* [†]	14.6±1.6	2.5-20.5
Torque peak	T_{max}	[Nm]	348±47*	378±26* [†]	297±23*	272-427
		[Nm·kg ⁻¹]	4.3±0.3*	4.4±0.3 [†]	4.1±0.1*	3.9-4.9
Time to torque peak	t_{Tmax}	[s]	0.392±0.229	0.436±0.193	0.317±0.275	0-0.67
Power peak	P_{max}	[W]	3047±646*	3419±507* [†]	2414±199*	2122-4199
		[W·kg ⁻¹]	37.4±4.9*	40±4.4* [†]	33.1±1.4*	30.5-45.2
Time to power peak	t_{Pmax}	[s]	1.237±0.229	1.304±0.248 [†]	1.122±0.138	0.96-1.7

Table 4.5: Dependent variable (t_{start}) and the general independent variables.* significantly strong correlation with t_{start} . [†] significant between-gender difference ($P < 0.05$). [‡] significant between-gender difference ($P < 0.001$)

Using absolute data: P_{max} is highly correlated with W_{top} , W_{bottom} and T_{max} ($r > 0.9$), also T_{max} is highly correlated with W_{top} . To avoid violating statistical assumptions underlying the stepwise regression analyses V_i , m_b and P_{max} were used as input in the predictive model for the dependent variable (t_{start}), V_i and P_{max} ended up in the model:

$$t_{start} = 2.8898 - 0.038113 \cdot V_i - 7.4029 \cdot 10^{-5} \cdot P_{max} \quad (4.2)$$

With model performance parameters: $RMSE = 0.274$, $R_{Adj}^2 = 0.845$, p-value = $7.43 \cdot 10^{-11}$. Shapiro-Wilk normality test gives a p-value of 0.4771, which is well above 0.05.

Using ratio scaled data The regression equation becomes:

$$t_{start} = 3.1451 - 0.039527 \cdot V_i - 0.0041503 \cdot m_b - 0.0038815 \cdot P_{max} \quad (4.3)$$

With model performance parameters: $RMSE = 0.0255$, $R_{Adj}^2 = 0.867$, p-value = $7.9 \cdot 10^{-11}$. Shapiro-Wilk normality test gives a p-value of 0.919, which is well above 0.05.

4.5.2 Pedalling variables

Descriptive data of the pedalling variables is presented in table 4.6 and 4.7 for all trials and for male (n=17) and female (n=10) trials separately. The relation between the general variables and the starting time is presented in Figure 4.9 and Figure 4.10.

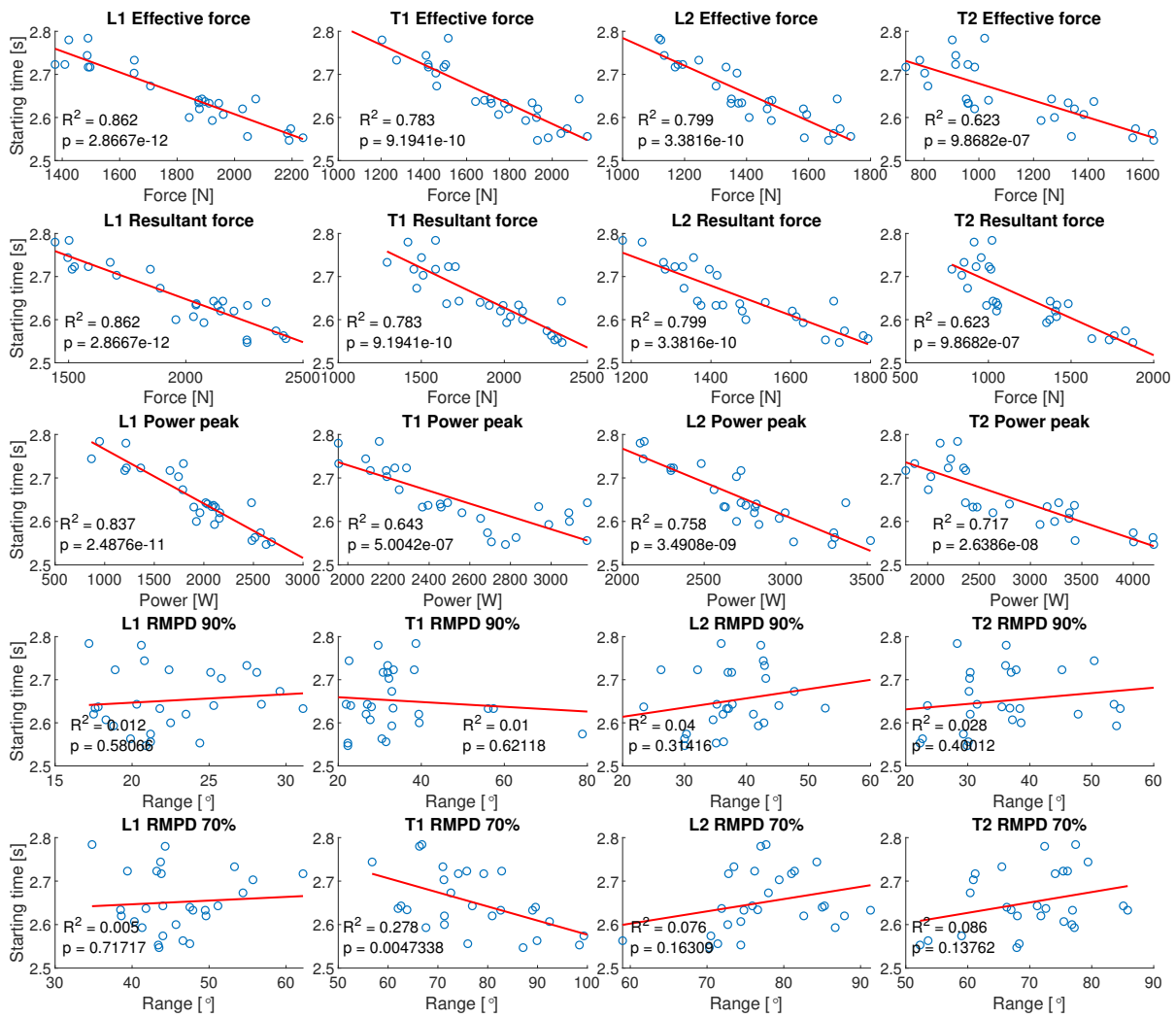


Figure 4.9: Relationship between pedalling variables and starting time (1)

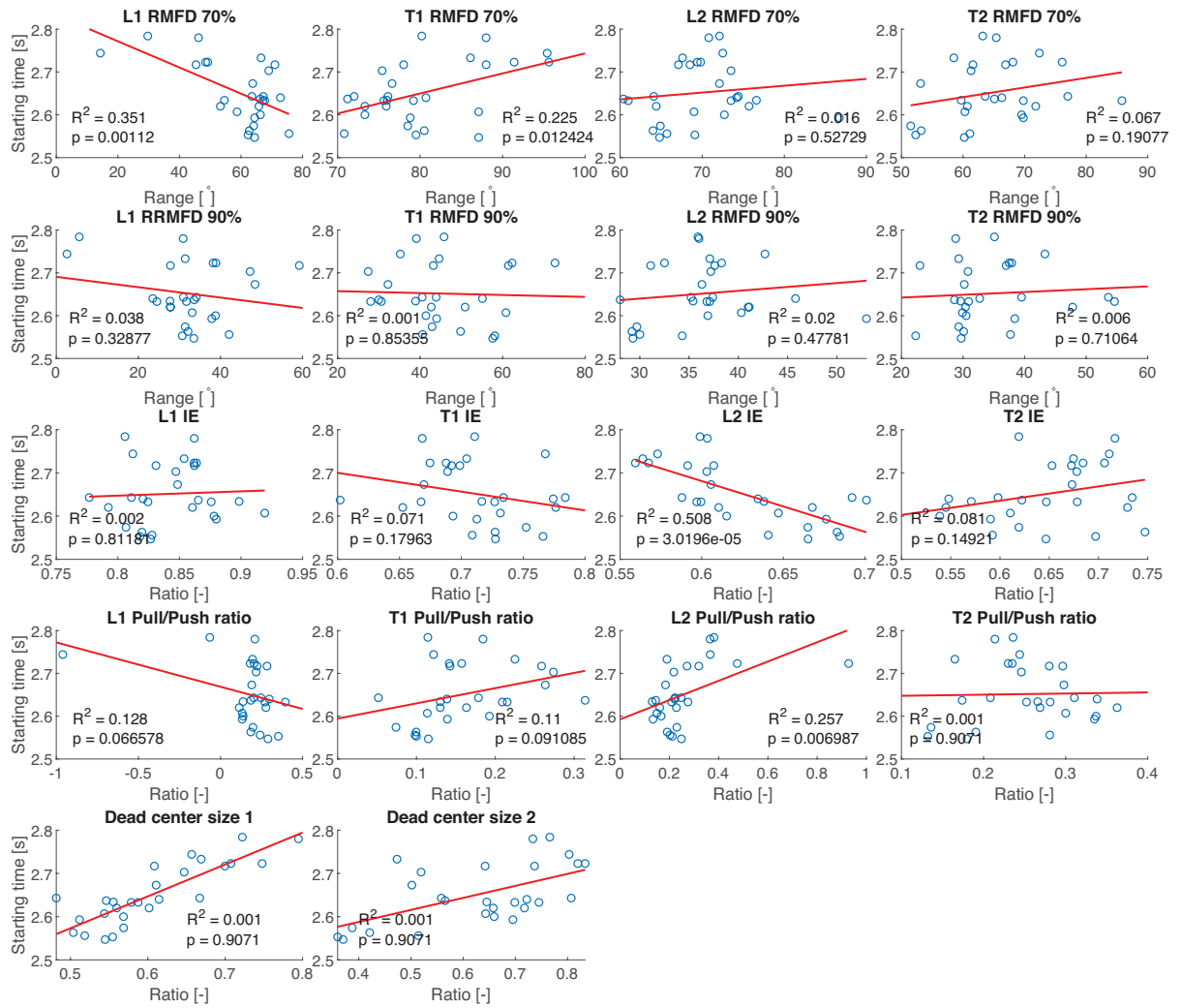


Figure 4.10: Relationship between pedalling variables and starting time (2)

Strength pedalling variables			All	Male	Female	range
Effective force peak	L1- Fe_{max}	[N]	1820±266*	1997±134*†	1518±113*	1375-2238
		[N·kg ⁻¹]	22.5±1.6*	23.4±1.1†	20.8±0.9	19.2-25.9
	T1- Fe_{max}	[N]	1710±269*	1884±159*†	1415±101*	1204-2164
		[N·kg ⁻¹]	21.1±2.1*	22.1±1.6†	19.5±1.9	16.3-24.6
	L2- Fe_{max}	[N]	1414±194*	1530±134*†	1217±91*	1117-1736
		[N·kg ⁻¹]	17.5±1.1*	17.9±1.1†	16.7±0.5*	16-20.3
T2- Fe_{max}	[N]	1138±280*	1288±240*†	883±95*	733-1640	
	[N·kg ⁻¹]	14±2.7*	15.1±2.6*†	12.2±1.9	9.4-18.1	
Resultant force peak	L1- Fr_{max}	[N]	1980±318*	2193±143*†	1619±156*	1442-2427
		[N·kg ⁻¹]	24.4±2.1*	25.7±1.1†	22.2±1.1*	20.7-27.7
	T1- Fr_{max}	[N]	1871±330*	2078±215*†	1519±121*	1294-2348
		[N·kg ⁻¹]	23.1±2.7*	24.4±2†	20.9±2.6	16.6-26.9
	L2- Fr_{max}	[N]	1479±179*	1578±144*†	1311±72*	1178-1794
		[N·kg ⁻¹]	18.3±1.2	18.5±1.3	18±1	16.2-20.8
T2- Fr_{max}	[N]	1221±334*	1400±294*†	918±82*	779-1874	
	[N·kg ⁻¹]	15±3.1*	16.4±3*†	12.7±1.8	10-20.2	
Power peak	L1- P_{max}	[W]	1915±510*	2231±265*†	1380±347*	867-2682
		[W·kg ⁻¹]	23.4±4.5*	26.1±1.9*†	18.7±3.8*	12.5-28.8
	T1- P_{max}	[W]	2528±380*	2755±280†	2141±116*	1953-3178
		[W·kg ⁻¹]	31.3±3.8	32.4±4†	29.5±2.5	25.1-39.4
	L2- P_{max}	[W]	2749±393*	2969±284*†	2374±231*	2107-3520
		[W·kg ⁻¹]	33.9±2.1*	34.8±1.9†	32.5±1.6*	30.3-37.8
T2- P_{max}	[W]	2843±738*	3265±594*†	2126±198*	1787-4199	
	[W·kg ⁻¹]	34.9±6.9*	38.1±6.1*†	29.4±4.2	22.9-45.2	

Table 4.6: Strength pedalling variables (1). * significant correlation with t_{start} . † significant between-gender difference ($P < 0.05$). # significant between-gender difference ($P < 0.01$). ‡ significant between-gender difference ($P < 0.001$). L1 = first pedal stroke lead leg, T1 = first pedal stroke trail leg, L2 = second pedal stroke lead leg, T2 = second pedal stroke trail leg. DC_1 = dead center size of the first pedal stroke from the lead and trail leg, DC_2 = dead center size of the second pedal stroke from the lead and trail leg.

Technical pedalling variables			All	Male	Female	range
Above 90% of F_e peak	L1-RMFD ₉₀	[°]	32±11	32±5	33±18	3-59
	T1-RMFD ₉₀	[°]	45±12	44±10	46±15	27-73
	L2-RMFD ₉₀	[°]	36±5	37±7	36±3	28-53
	T2-RMFD ₉₀	[°]	34±8	35±9	33±6	22-55
Above 70% of F_e peak	L1-RMFD ₇₀	[°]	59±14 *	65±6 [†]	50±18	14-76
	T1-RMFD ₇₀	[°]	80±7	77±5 [†]	85±8	71-96
	L2-RMFD ₇₀	[°]	70±6	69±7	70±2	60-87
	T2-RMFD ₇₀	[°]	65±8	65±9*	65±7	52-86
Above 90% of power peak	L1-RMPD ₉₀	[°]	22±4	22±4	24±4	17-31
	T1-RMPD ₉₀	[°]	34±12	35±15	32±4*	22-79
	L2-RMPD ₉₀	[°]	38±7	37±7	39±6	23-53
	T2-RMPD ₉₀	[°]	36±9	36±11	36±7*	22-55
Above 70% of power peak	L1-RMPD ₇₀	[°]	46±6	45±4	47±8	35-62
	T1-RMPD ₇₀	[°]	77±11*	80±12	72±7	57-99
	L2-RMPD ₇₀	[°]	77±7	77±8*	78±4	59-91
	T2-RMPD ₇₀	[°]	70±9	70±9*	70±7	52-86
Index of force effectiveness	L1-IE	[-]	0.84±0.03	0.84±0.04	0.84±0.02	0.78-0.92
	T1-IE	[-]	0.71±0.04	0.72±0.05	0.70±0.03	0.60-0.78
	L2-IE	[-]	0.63±0.04*	0.65±0.04 [‡]	0.59±0.02*	0.56-0.70
	T2-IE	[-]	0.65±0.06	0.63±0.07 [†]	0.68±0.03	0.54-0.75
Push Pull ratio	L1-PP	[-]	0.17±0.24	0.22±0.08	0.07±0.37	-0.96-0.39
	T1-PP	[-]	0.16±0.07	0.14±0.06	0.19±0.06	0.05-0.31
	L2-PP	[-]	0.26±0.16*	0.20±0.04 [#]	0.37±0.22	0.13-0.93
	T2-PP	[-]	0.25±0.06	0.26±0.07	0.24±0.04	0.13-0.36
Dead center size	DC ₁	[-]	0.61±0.08*	0.56±0.04 [‡]	0.69±0.06*	0.48-0.79
	DC ₂	[-]	0.63±0.14*	0.60±0.14*	0.68±0.14*	0.36-0.83

Table 4.7: Technical pedalling variables (2). * significant correlation with t_{start} .[†] significant between-gender difference ($P < 0.05$).[#] significant between-gender difference ($P < 0.01$). [‡] significant between-gender difference ($P < 0.001$). L1 = first pedal stroke lead leg, T1 = first pedal stroke trail leg, L2 = second pedal stroke lead leg, T2 = second pedal stroke trail leg. DC₁ = dead center size of first crank revolution, DC₂ = dead center size of second crank revolution.

Using absolute data: Only the variables with significantly strong correlation with t_{start} were considered for the model. To avoid violating statistical assumptions underlying the stepwise regression analyses power peak, resultant force peak were excluded from the model because of the high correlation with effective torque. L2- $F_{e_{max}}$ was excluded because of its high correlation with L1- $F_{e_{max}}$. V_i , L1- $F_{e_{max}}$, T1- $F_{e_{max}}$, T2- $F_{e_{max}}$, T1-RMPD₇₀, L2-IE, L2-PP, DC₁ and DC₂ were used as input in the predictive model for the dependent variable (t_{start}). V_i , L1- $F_{e_{max}}$, T1- $F_{e_{max}}$ and T1-RMPD₇₀ ended up in the model:

$$\begin{aligned}
 t_{start} = & 3.0666 - 0.033698 \cdot V_i - 1.0066 \cdot 10^{-4} \cdot L1F_{e_{max}} \\
 & - 7.4454 \cdot 10^{-5} \cdot T1F_{e_{max}} - 1.2137 \cdot 10^{-3} \cdot T1RMPD_{70}
 \end{aligned} \tag{4.4}$$

With model performance parameters: $RMSE = 0.0203$, $R^2_{Adj} = 0.915$, $p\text{-value} = 2.99 \cdot 10^{-12}$. Shapiro-Wilk normality test gives a p-value of 0.1364, which is well above 0.05.

Using power peak over effective force peak, the regression equation becomes:

$$t_{start} = 3.0205 - 0.033357 \cdot V_i - 5.5069 \cdot 10^{-5} \cdot L1P_{max} - 5.2495 \cdot 10^{-5} \cdot T1P_{max} - 1.5549 \cdot 10^{-3} \cdot T1RMPD_{70} \quad (4.5)$$

With model performance parameters: $RMSE = 0.0183$, $R^2_{Adj} = 0.931$, $p\text{-value} = 3.14 \cdot 10^{-13}$. Shapiro-Wilk normality test gives a p-value of 0.7596, which is well above 0.05.

Using ratio scaled data When using effective force peak over power peak the regression equation becomes:

$$t_{start} = 2.5649 - 0.039837 \cdot V_i - 0.0022431 \cdot T1RMPD_{70} + 0.44949 \cdot DC1 \quad (4.6)$$

With model performance parameters: $RMSE = 0.0259$, $R^2_{Adj} = 0.862$, $p\text{-value} = 1.22 \cdot 10^{-10}$. Shapiro-Wilk normality test gives a p-value of 0.4728, which is well above 0.05.

When using power peak over effective force the regression equation becomes:

$$t_{start} = 2.738 - 0.030117 \cdot V_i - 0.0051786 \cdot T1P_{max} - 0.0017161 \cdot T1RMPD_{70} + 0.2914 \cdot DC1 \quad (4.7)$$

With model performance parameters: $RMSE = 0.0226$, $R^2_{Adj} = 0.895$, $p\text{-value} = 2.96 \cdot 10^{-11}$. Shapiro-Wilk normality test gives a p-value of 0.3533, which is well above 0.05.

In the regression equation of pedalling performance variables only variables from the first pedal stroke of the lead and trail leg appear. Figure 4.11 present the effective force of one cyclist for the first pedal stroke of the lead leg (in red) and trail leg (in blue).

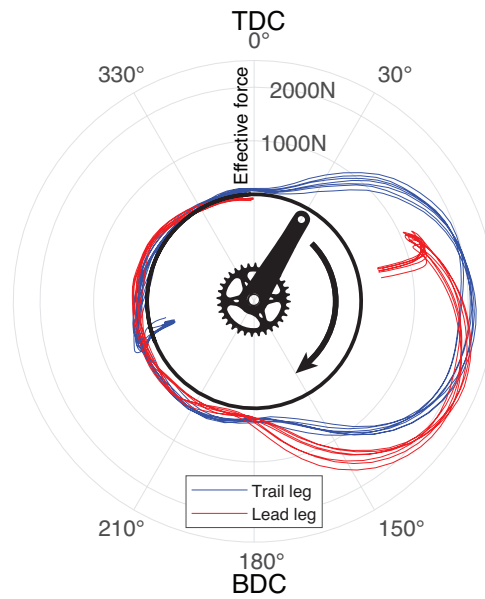


Figure 4.11: Effective force [N] of the first pedal stroke from the lead leg (red) and trail leg (blue) from all trials of one participant.

It can be seen from Figure 4.11 that the initial position of the cranks is between 80° and 90° for the lead leg. During the preparation movements, i.e. sling shot maneuver the effective force of both the lead and trail leg drops. The lead leg reaches its maximum effective force around 120° . Thereafter the pull back of the lead leg in the BDC area and at the same time the set up of the trail leg in the TDC area, both contributing to a high dead center size (DC1). After the set up of the trail leg it can be seen a high effective force is reach early in the crank cycle by the trail leg, around 50° . The trail leg is able to maintain a high effective force for a long duration in the push phase, hence a high relative maximum power duration ($RMPD_{70}$). Furthermore, during the pull phase (between 210° and 330° the effective force remains positive, i.e. there is a active pull of both lead and trail leg and is positively contributing to propulsion of the bicycle.

4.6 Participants subjective performance assessment

The result of the subjective score participant give to their starting performance after every trial is presented in Figure 4.12.

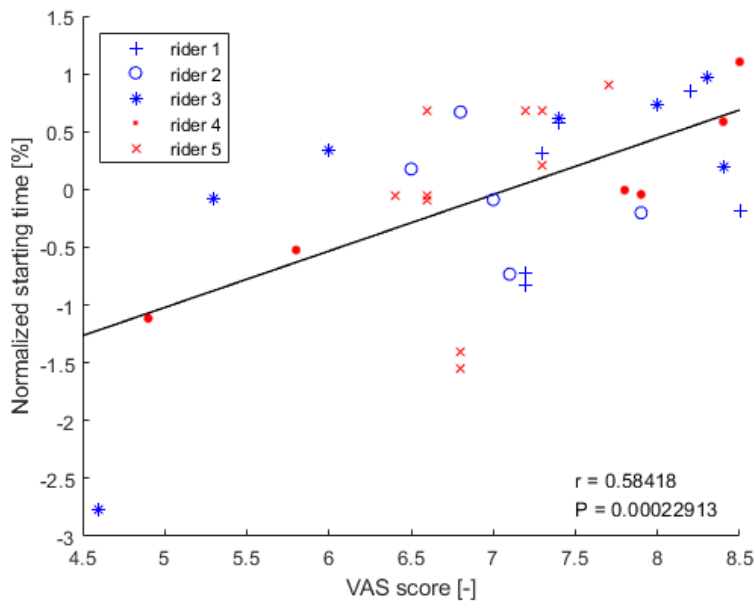


Figure 4.12: Relationship between VAS score of participants and starting time. Blue = Male participants, red = female participants. Black line is the linear regression line. r = Pearson correlation and P = p-value for statistical significance.

Starting times are normalized to percentage difference from the mean starting time of a participant. There is a significant strong correlation between participant assessment of their performance with starting time ($r=0.58, P<0.001$). Furthermore, there were no statistically significant differences between participants as determined by one-way ANOVA ($F(4,30) = 0.647, p = 0.63$). The performance assessment of rider 3 and 4 show a positive correlation with their performance (S3: $r = 0.76, n = 7, p = 0.048$, S4: $r = 0.92, n = 6, p = 0.009$). Moreover they have a larger bandwidth of assessing their performance. There was no statistically significant correlation between VAS score and normalized performance for the other riders (S1: $r = 0.38, n = 6, p = 0.453$, S2: $r = -0.46, n = 6, p = 0.353$, S5: $r = 0.44, n = 10, p = 0.199$)

Chapter 5

Discussion and implications

Study objectives and major findings

The objective of this study was to (1) gain more insight in the performance of BMX racing as in how a cyclist effectively propel the bicycle during a BMX gate start, and (2) identify pedalling performance predictors of a fast start. Key was the field-based collection of enriched pedal force data of world class athletes on a supercross start hill. The use of an instrumented crank (Axis2d, Swift Performance, Brisbane, AU) made it possible for the first time to analyse pedalling mechanical effectiveness outdoors.

For the first objective 60% of the total work by a BMX cyclist is done in the first 5 meters of the start, explaining over 90% of the variation in starting time (t_{start}). For the second objective, the results of this survey suggests two strength related variables and two technical related variables to be good predictors of a fast gate start in BMX racing. The strength related predictors are power peak of the first and second pedal stroke ($L1-P_{max}$ and $T1-P_{max}$). In addition to the initial velocity at the gate drop (V_i) the second technical predictor that is identified in this study is the Relative Maximal Power Duration of the second pedal stroke ($RMPD_{70}$). These four variables explain 89-93% of the variation in starting time. Moreover, according to the results of this study time to peak power ($t-P_{max}$), index of force effectiveness (IE) and Push Pull ratio (PP) could not be identified as good predictor of performance in BMX racing.

Meaning and importance

Since starting time is crucial to obtain an advantageous position to lead the race and its impact on race results [1] these findings suggest 90% of the race is decided after 5 meters into a race. Apart from the obvious strength variable, power peak, some additional technical pedalling variables provide more insight in the BMX start performance, and could be included in assessment of performance during training or racing. Furthermore, the results reveal the major opportunities for improvement of the starting time can be found in the first crank revolution. The identified performance predictors can be quantified without radial force data, meaning instrumentation capable of collection torque and crank angle data alone could be sufficient for performance assessment of the BMX start. When V_i , P_{max} of the first two pedal strokes and $T1-RMPD_{70}$ would improve by 5% the starting time would decrease with 0.70% for absolute data and 0.60% for ratio scaled data, i.e the cyclist would be ahead by 13-15 cm, a worthwhile chance.

5.1 Ecological validity

Mass scaling

Where allometrically scaled data (scaled by body mass^{2/3} [29] [28]) were not significantly different from absolute data, ratio scaled data showed significant difference in correlation with starting time when compared with absolute data. Measured "body mass" included protective gear, helmet and shoes, over estimating real body mass with approximately 5%. However, correcting for this over estimation reveals the same results in correlation differences.

Body mass has a negative correlation with starting time ($r = -0.833, p < 0.001$) and also appears with a negative coefficient in the regression equation (equation 4.3) meaning an increase in mass will enhance starting time. Furthermore, when scaling the strength related variables with body mass the correlations with starting time become weaker, indicating the inter correlation between body mass and strength (i.e. power and force production). However, the normalised strength variables keep a high correlation with starting time. Considering these results we can conclude the slope of the starting hill and the power production of the athletes outweigh the negative affect of increased inertia during the start with increased body mass. It would be advised to use ratio normalised data over absolute data to exclude the affect of mass on the strength related results during pedalling performance analyses. So strength can be assessed independent of body mass, for example during performance monitoring and comparing results with a benchmark or comparing between athletes.

First versus second pedal stroke

There is a highly significant between participant difference for the movement time of the first and second pedal stroke. The result revealed only a significant between-gender difference for the first pedal stroke ($P < 0.001$). The male first pedal stroke is slower compared to female participants (0.414 ± 0.010 and 0.352 ± 0.039 [s] respectively). The higher body mass, i.e higher inertia, for the male participants makes it more difficult to accelerate from a standstill, despite the slingshot maneuver. Additionally, the majority of male participant used a bigger rear wheel (5cm larger wheel circumference) to mimic their preferred gear ratio. Nevertheless, male participants were able to have a faster second pedal stroke than female participants (0.341 ± 0.008 and 0.387 ± 0.025 [s] respectively). This could imply that these male participants more than compensate higher mass with their ability to produce greater power during the second pedal stroke.

Initial velocity

Overall participants were able to produce positive initial velocity (0.33 ± 0.56 [m/s]). The initial velocity is defined as velocity when the gate drops, and not when the green light illuminates. The moment of initiation of forward velocity often lies within the interval between illumination of the green light and the gate drop (interval 0.06-0.07 seconds). Delay of the gate drop might be due to inertia of the pneumatic cylinder and the gate, since the start pulse is sent to the light and the gate simultaneously by the timing system. It is speculated BMX cyclist

time on the gate rather than on the light, since close gate clearance is crucial. In discussion with some riders, some mentioned that they focus on the light, others on the gate, so there seems to be a difference in strategy for timing gate starts.

The appearance of initial velocity in the regression equations and its negative correlation with starting time ($r = -0.781$, $p\text{-value} < 0.001$) demonstrates the importance of a positive velocity when the gate drops. The results show that female participant more often have a negative velocity when the gate drops, i.e. bike still moving backwards, compared to male participants. There is a thin balance between establishing a high positive initial velocity and prevent hitting the gate when performing the slingshot maneuver before the gate drop. Nevertheless, timing of the slingshot so that initial velocity increases could further improve start performance.

Work done before versus work done after the kink

The gradient of the cumulative work is larger for the traveled distance up to kink than it is after the kink (see Figure 4.7), indicating more work per meter is done at the beginning of the start than at the steeper section of the ramp, i.e. a rider is able to generate more work at low velocity and less slope than at higher velocities and steeper slope. The high portion of work done before the kink (60%) and its high correlation with starting time ($r = -0.952$, $p\text{-value} < 0.001$) concludes to focus on pedalling performance during this section of the start. Up to the kink four pedal strokes are performed, analyses on pedalling performance is therefore conducted on the first four pedal strokes of the BMX start.

Up to the kink the cumulative work has an erratic behavior, indicating larger difference in generated work within a pedal stroke. The near horizontal gradient parts up to the kink indicate the dead centers within a pedal stroke where almost no work is generated. This could be due to a low crank rotational velocity or a low torque production. Presenting cumulative work could help identify difference between cyclist and within cyclist difference over time. It could help identify areas for potential improvements and gain insight in general performance as well as benchmarks during training periods.

The smaller the shaded area around the solid line of a rider the lower the standard deviation is. This means a rider has been more consistent in work production over his trials during the experiment, rider 2 for example shows to be very consistent in work production. Riders differ in when they stop pedalling, rider 1 stops last of all riders which is one of the reasons that rider has a higher total work over the start.

Sections of crank revolution

The crank revolution can be divided in sections in different manners, as can be seen in Figure 5.1. Some literature uses 90° quadrants (a) [33] [2], others four sections from $0 \pm 45^\circ$ (b) [33]. In flat ground cycling TDC and BDC are statically positioned in 0° and 180° respectively, but in BMX starts they are more dynamic. Up to the kink the slope of the ramp is 15° and during the first four pedal strokes of the BMX start the cyclist pulls up their front wheel, this will cause the TDC and BDC to deviate from their vertical position. Additionally, the

hip movements of the cyclists will further tilt the dead centers. This hip movement enables the cyclist to lengthen their push phase during the pedal stroke. In line with this reasoning, analysing the pedal forces (Figure 4.3) the push and pull phases during the BMX start are more realistically reflected when defined as 30° - 150° and 210° - 330° sections respectively (Figure 5.1 (c)). Furthermore, reflecting the TDC and BTC areas as $0^\circ \pm 30^\circ$ and $180^\circ \pm 30^\circ$ respectively guaranties the dead centers will be within this regions throughout the BMX start.

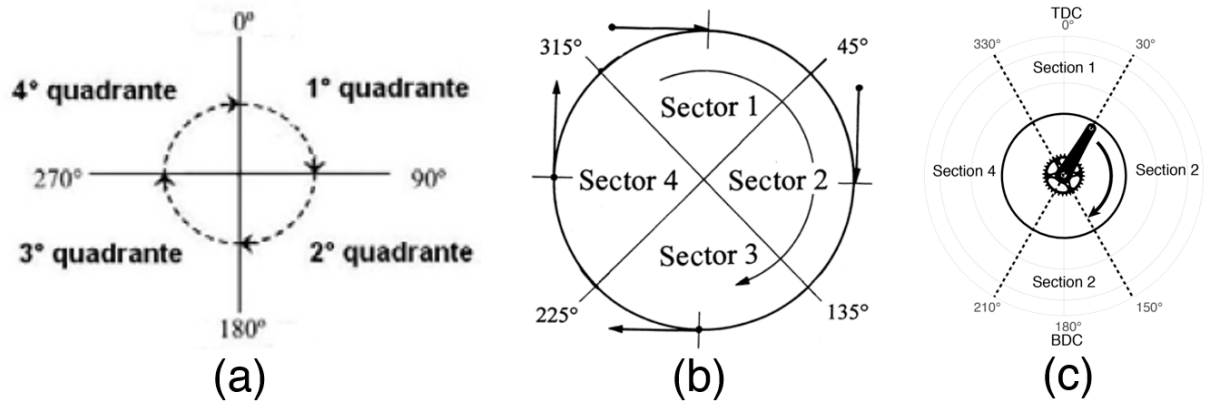


Figure 5.1: Crank revolution division in sections. (a) quadrants of 90 degree from TDC (0°) [33] [2], (b) four sections from $0 \pm 45^\circ$ [33] and (c) four sections with $0^\circ \pm 30^\circ$, $180^\circ \pm 30^\circ$.

Peddalling performance predictors

Power peak is reached after 1.237 ± 0.229 seconds, mostly in the fourth pedal stroke and sometime in the third pedal stroke. From absence of any pedalling variables within the third and fourth pedal stroke in the regression equations 4.4, 4.5, 4.6 and 4.7 we can conclude the first two pedal strokes are more important for a fast gate start than the latter two, despite the fact overall power peak is reached in the latter pedal strokes. It does not make overall power peak unimportant; there is a high inter correlation between power peak of the first pedal stroke and the overall power peak ($r = 0.918$). It means power peak of the first pedal stroke already provides enough information for a good prediction of starting time.

Appearance of pedalling variables P_{max} , Fe_{max} and $RMPD_{70}$ for the second pedal stroke in the regression equations indicate the importance of the second pedal stroke. Apart from generating a high peak force and peak power the duration in which a high power production is maintained is of importance, quantified by $RMPD_{70}$. Cyclists constantly drive their hips forward towards the handle bar for every pedal stroke up to the kink, it is hypothesised this hip movement facilitated the ability to generate high force close to the BTC for the lead leg, seen in Figure 4.11. Furthermore, it can be hypothesised that bringing their hips back behind the saddle for the following pedal stroke would enable the cyclist to generate high effective force right after the TDC for the trail leg. The technical variable $RMPD_{70}$ could therefore potentially be used to quantify the effectiveness of this hip movement and help coaches to

identify where improvements for performance are possible.

Moreover, the appearance of DC1 in the regression equations using scaled data 4.6 and 4.7 indicated the importance of the dead center size. However, DC1 appear to be positively correlated with starting time, meaning an increased dead center size results in a slower starting time. This is contrary to what was hypothesised. The parameter describes the evenness of work rate generation and would result in lower repetitive deceleration of a cyclists inertia during the sprint, which might be beneficial during BMX gate starts. This positive coefficient can be explained by the significant between-gender difference of DC1 (0.56 for male, 0.69 for female). For male riders DC1 had no strong correlation with starting time ($r=0.41$, $p>0.1$), but for female cyclist there was a strong positive correlation ($r=0.79$, $p<0.05$). Furthermore, there is an even stronger significant between-gender difference for P_{max} in the first two pedal strokes. Since DC1 was defined as work rate in the dead center areas divided by average work rate over the crank revolution, the presence of DC1 with a positive coefficient in the regression model tells more about the absence of high average power for the female cyclist then the presence of high work rate in the dead centers. It does indicate female participants were better able to generate a more even work rate generation over the first two pedal strokes then male participants.

Subjective score

The participants were asked to assess their own performance (VAS score) during the measurements to investigate how well this self assessment could reflect actual starting time performance (t_{start}). The results show a positive correlation between normalised starting time and VAS scores. Two participants were well capable of assessing their performance before knowing their starting time, i.e. strong correlation between VAS assessment and normalised starting time (S3: $r = 0.76$, $n = 7$, $p = 0.048$, S4: $r = 0.92$, $n = 6$, $p = 0.009$). When asked to comment why a particular start was good or bad, participants comment were in line of 'good timing', 'bad gate exit' or 'better acceleration'. The identified predictors could assist cyclists by providing an objective insight next to the subjective assessment and thereby help to better interpret and understand individual performance.

5.2 Comparison with other literature

Power

Present study reports peaks of continuous power (P_{max}) of 3047W, $37.4W \cdot kg^{-1}$ for all participant. For comparison with other literature the male group reported 3419W, $40W \cdot kg^{-1}$. Other literature only report peak power as average power over pedal strokes. Peak average power over pedal strokes in the present study for all participants (1914 ± 270 , $23.7W \cdot kg^{-1}$) and for male specifically (2048 ± 205 , $24W \cdot kg^{-1}$), was higher then for male cyclist (1810 W, $23.6 W \cdot kg^{-1}$, $n=10$) studied by Gross et al. [3] but comparable to the values reported by Herman

et al. [10] ($2087 \pm 156.8W$, $n=5$) for male cyclists. Both field based studies were conducted on a BMX SX starting hill with elite BMX cyclists.

In field based studies not conducted on a SX starting hill lower power peaks are reported. On a 5m high start ramp Rylands et al. [21] report $1671 \pm 188W$, $24W \cdot kg^{-1}$ peak power values (SRM 0.5Hz, elite male $n=8$). Flat ground sprint tests result in peak power recordings of $1631 W$, $23.5 W \cdot kg^{-1}$ (Powertap 0.8Hz, male $n=5$, female $n=2$) [19] and $1539 \pm 148W$, $21.29 \pm 0.84W \cdot kg^{-1}$ (SRM 0.5Hz, elite male $n=5$) [34].

In laboratory based studies the lowest values are reached. Rylands et al. [35] reported $1105 \pm 139W$, $16.25W \cdot kg^{-1}$ (SRM ergometer 2Hz, elite male $n=6$) and Janssen & Cornelissen [12] reported $1329 \pm 163W$, $18W \cdot kg^{-1}$ (Wattbike 100Hz, junior male $n=3$ and junior female $n=2$).

It is notable peak power values increase when the test environment becomes more comparable with BMX training and race environment, it shows the importance of conducting measurements in an ecological valid environment. A second explanation is that in some of these studies the only instrumentation available at that time collect data at a low sample rate (0.8 - 2Hz) which may have resulted in potentially missing crucial pedalling performance parameters of the highly dynamic and fast BMX start.

Index of Effectiveness

Results in the present study on Index of Effectiveness show higher values for the first two pedal strokes than the latter ($L1=0.84$, $T1=0.71$ over $L2=0.63$, $T2=0.65$ respectively), this is in line with findings from Janssen & Cornelissen [12] reporting IE for BMX cyclists of 0.76 and 0.77 for the first pedal stroke of the lead and trail leg respectively and 0.55 for both the second pedal stroke of the lead and trail leg.

IE values in the present study are higher than those of Janssen & Cornelissen possibly due to laboratory setting of the measurements (Wattbike ergometer). Furthermore, results might also be affected by choosing junior BMX cyclists, whereas in present study only elite BMX cyclists participated.

Relative Maximum Power Duration

Bertucci et al. [13] reported Relative Maximum Power Duration (RMPD) over the first three pedal strokes. Relative Maximum Power Duration when power output exceeds 90% in this study report lower values (33.1° average over first three pedal strokes for male) compared to the work of Bertucci et al. ($RMPD_{90} = 46.1^\circ$ and 56° for regional and elite cyclist respectively). Relative Maximum Power Duration when power output exceeds 70% (67.3°) was lower compared to Bertucci et al. ($RMPD_{70} = 84.6^\circ$ and 90.9° for regional and elite cyclist respectively). It is difficult to draw any conclusions from these differences because the nature of the studies were so different. Bertucci et al. used cyclo-cross cyclists as participants in a laboratory based study using a SRM ergometer measuring torque at 250Hz (compared to 100Hz in current

study), but mean crank angular velocity over a crank revolution for the calculation of power output.

5.3 Limitation

Results in this study are based on 27 gate start trials divided over five elite BMX cyclists. This limited the maximum number of selected independent variables for the regression models to 3-4 as a rule of thumb. Nevertheless, p-values below the significance threshold of 0.05 were found for the presented predictors. However, when the sample size is small a more conservative approach can be advised to avoid Type 1 errors (concluding that a variable has an effect when it really doesn't) by using a significance threshold one level stricter (p-value < 0.01) to increase confidence in the found predictors [36]. In absolute and ratio scaled regression models V_i , P_{max} , T1-RMPD₇₀ and DC1 all had significant levels below 0.01 (see Appendix D). Although the smaller sample size will lead to increased error margins, the results do imply an indication of performance, and even a strong indication for the predictor variables with a significance level below 0.01.

Due to practical limitations 100Hz sample frequency for data collection was used, despite the fact the instrumented cranks are capable of collecting data at 200Hz. Data collection with 100Hz still provides 25 to 75 data points for every pedal stroke up to the kink, therefore there is reason to believe the main conclusions in this work would remain unchanged when data collection would have been conducted at 200Hz. Furthermore, a custom data acquisition device (DAQ) has been developed capable of collecting data at 200Hz in future research.

And finally, this study did not consider the 'pumping' maneuver in the transition zone at the end of the starting hill. As also mentioned by Gross et al. [3] this pumping maneuver: *"similarly to a skateboarder in the halfpipe, riders can increase system energy by a vertical movement of their center of mass and, in this manner, potentially accelerate the bike independently of pedaling power (Rylands et al. 2017 [35])"*.

5.4 Practical relevance

In the BMX start a cyclist who is ahead by 10 cm at the bottom of the start hill has the advantage. This difference would allow the cyclist to move his or her wheel in front of its competitors to obtain an advantageous position to lead the race. Using the mean velocity over all trials in this study this 10 cm difference in distance translates into a time difference in starting time of 0.012 seconds, which is 0.45% of the mean starting time. When V_i , P_{max} of the first two pedal strokes and T1-RMPD₇₀ would improve by 5% the starting time would decrease with 0.70% for absolute data and 0.60% for ratio scaled data, i.e the cyclist would be ahead by 13-15 cm, a worthwhile chance.

Chapter 6

Conclusion

6.1 Conclusion

The objective of this study was to (1) gain more insight in the performance of BMX racing as in how a cyclist effectively propels the bicycle during a BMX gate start, and (2) identify pedalling performance predictors of a fast start. Key was the field-based collection of enriched pedal force data of world class athletes on a supercross start hill.

A high initial velocity (V_i) is required for an advantageous acceleration in the gate start. It has been found 60% of the total work by a BMX cyclist is done in the first 5 meters of the start, explaining 90% of variation in starting time, making this the most important section of the start. Peak effective force (Fe_{max}) and power (P_{max}) of the first two pedal stroke supplemented with technical variable $RMPD_{70}$ over the second pedal stroke are good predictors of performance in BMX, together they explain 89-93% of the variation in starting time, hence quantifying pedal forces provides more insight in gate start performance during BMX cycling. These findings suggest opportunities for improvement of the starting time can be found in the first crank revolution.

6.2 Practical application

A cyclist could (1) focus on an effective slingshot maneuver to increase bicycle velocity at the gate drop, (2) improve maximum power output in the first two pedal strokes and (3) focus on extending the range of high power output in the second pedal stroke, i.e the trail leg. The identified performance predictors P_{max} , Fe_{max} , $RMPD_{70}$ can be quantified without radial force data, meaning instrumentation capable of collection torque and crank angle data alone could be sufficient for performance assessment of the BMX start in daily use.

6.3 Recommendations and future outlook

Firstly, by monitoring pedalling performance over a period of time in the near future would allow to verify if conclusion from present study will also hold for larger data sets. Additionally, incorporating the build DAQ in daily training environment would further ease the collection and processing of data. Moreover, the setup would be less susceptible for data package loss through wireless transmission since the DAQ would be close to the crank at all times with a clear line-of-sight when attached to the handlebar. Ultimately leading to a feedback system capable of assisting coaches during gate start training in providing feedback to their athletes.

Secondly, in order to further understand the relationship between hip movement and transfer of force onto the pedals, additional research could investigate this relationship in the future. A unique set of both 3D kinematics (3D motion capture suits, Xsens) and pedal force data have been collected during present study and could be used for analyses.

Thirdly, investigations could move from observational study to an experimental research. For example investigating interventions on gear ratio, warm-up routine, movement patterns or pedal orientation in relationships with starting performance.

Lastly, the scope of present study could be expanded to other cycling disciplines such as track sprint and road sprinting to investigate the influence of the pedalling performance variables on performance in those fields. Furthermore, the use of the instrumented cranks in present study could be expand to the field of rehabilitation, it might be useful in rehabilitation research for monitoring left and right leg differences after injury.

Chapter 7

Acknowledgement

I would like to thank my supervisors, Dr. Daan Bregman, Dr. Ina Janssen and Dr. Ir. Arend Schwab, for the opportunity and guidance throughout this project.

I would like to thank Raymon van der Biezen and Rob van den Wildenberg head coaches of the Duth BMX team for given the opportunity to conduct measurements and for sharing their knowledge of BMX cycling. Additional thanks goes out to Sportcentrum Papendal, Royal Dutch Cycling Union (KNWU), and the members of the Dutch BMX cycling team for their support and participation in experiments.

Finally, I would like to thank Meybo, in particular Willie Meijer, for their time and patience in the assembly of the experimental bicycle. DEMO, in particular Hans van der Does, for the electronic and mechanical support during this project and creation of the DAQ. And lastly Swift performance, in facilitating an instrumented crank for this project.

This research was financially supported by the Tokyo Innovation Fund of the TU Delft Sports Engineering Institute.

References

- [1] L. Rylands and S. J. Roberts, "Relationship between starting and finishing position in world cup bmx racing", *International Journal of Performance Analysis in Sport*, vol. 14, no. 1, pp. 14–23, 2014.
- [2] R. Bini, P. Hume, J. L. Croft, and A. Kilding, "Pedal force effectiveness in cycling: A review of constraints and training effects", 2013.
- [3] M. A. D. Gross, F. Schellenberg, G. Lüthi, M. Baker, and S. Lorenzetti, "Performance determinants and leg kinematics in the bmx supercross start", *Journal of Science and Cycling*, vol. 6, no. 2, p. 3, 2017.
- [4] J. C. Martin, C. J. Davidson, and E. R. Pardyjak, "Understanding sprint-cycling performance: The integration of muscle power, resistance, and modeling", *International journal of sports physiology and performance*, vol. 2, no. 1, pp. 5–21, 2007.
- [5] UCI. (). Constitutions and regulation, Union Cycliste Internationale, [Online]. Available: <https://www.uci.org/inside-uci/constitutions-regulations/regulations>. (accessed: 19.11.2018).
- [6] M. Kalichová, S. Hřebíčková, R. Labounková, P. Hedbávn, and G. Bago, "Biomechanics analysis of bicross start", *International Journal of Medical, Health, Pharmaceutical and Biomedical Engineering*, vol. 7, pp. 361–369, 2013.
- [7] M. Zabala, C. Sánchez-Muñoz, and M. Mateo, "Effects of the administration of feedback on performance of the bmx cycling gate start", *Journal of sports science & medicine*, vol. 8, no. 3, p. 393, 2009.
- [8] J. F. Cowell, J. B. Cronin, and M. R. McGuigan, "Time motion analysis of supercross bmx racing", *Journal of sports science & medicine*, vol. 10, no. 2, p. 420, 2011.
- [9] P. Debraux and W. Bertucci, "Determining factors of the sprint performance in high-level bmx riders", *Computer Methods in Biomechanics and Biomedical Engineering*, vol. 14, no. sup1, pp. 53–55, 2011.
- [10] C. W. Herman, S. J. McGregor, H. Allen, and E. M. Bollt, "Power capabilities of elite bicycle motocross (bmx) racers during field testing in preparation for 2008 olympics.: 2321", *Medicine & Science in Sports & Exercise*, vol. 41, no. 5, pp. 306–307, 2009.
- [11] I. Janssen, A. Oude Alink, and F. Frielink, "Elite bmx cyclists use individual strategies for a successful start", *ISBS Proceedings Archive*, vol. 36, no. 1, p. 126, 2018.
- [12] I. Janssen and J. Cornelissen, "Pedal forces during the bmx and track sprint cycling start", *ISBS Proceedings Archive*, vol. 35, no. 1, p. 277, 2017.

- [13] W. Bertucci, R. Taiar, Y. Toshev, and T. Letellier, "Comparison of biomechanical criteria in cycling maximal effort test", *Int J of Sports Sci Eng*, vol. 2, no. 1, pp. 36–46, 2008.
- [14] S. Leirdal and G. Ettema, "Pedaling technique and energy cost in cycling.", *Medicine and science in sports and exercise*, vol. 43, no. 4, pp. 701–705, 2011.
- [15] T. Korff, L. M. Romer, I. Mayhew, and J. C. Martin, "Effect of pedaling technique on mechanical effectiveness and efficiency in cyclists", *Medicine & Science in Sports & Exercise*, vol. 39, no. 6, pp. 991–995, 2007.
- [16] L. Rylands and S. Roberts, "Performance characteristics in bmx racing: A scoping review", *Journal of Science and Cycling*, vol. 8, no. 1, 2019.
- [17] M. Mateo, C. Blasco-Lafarga, and M. Zabala, "Pedaling power and speed production vs. technical factors and track difficulty in bicycle motocross cycling", *The Journal of Strength and Conditioning Research*, vol. 25, no. 12, pp. 3248–3256, 2011.
- [18] W. Bertucci, R. Taiar, and F. Grappe, "Differences between sprint tests under laboratory and actual cycling conditions", *Journal of sports medicine and physical fitness*, vol. 45, no. 3, p. 277, 2005.
- [19] P. Debraux, A. V. Manolova, M. Soudain-Pineau, C. Hourde, and W. Bertucci, "Maximal torque and power pedaling rate relationships for high level bmx riders in field tests", *Journal of Science and Cycling*, vol. 2, no. 1, p. 51, 2013.
- [20] W. M. Bertucci and C. Hourde, "Laboratory testing and field performance in bmx riders", *Journal of sports science & medicine*, vol. 10, no. 2, p. 417, 2011.
- [21] L. P. Rylands, S. J. Roberts, and H. T. Hurst, "Variability in laboratory vs. field testing of peak power, torque, and time of peak power production among elite bicycle motocross cyclists", *The Journal of Strength & Conditioning Research*, vol. 29, no. 9, pp. 2635–2640, 2015.
- [22] M. Freyd, "The graphic rating scale.", *Journal of educational psychology*, vol. 14, no. 2, p. 83, 1923.
- [23] M. E. Wewers and N. K. Lowe, "A critical review of visual analogue scales in the measurement of clinical phenomena", *Research in nursing & health*, vol. 13, no. 4, pp. 227–236, 1990.
- [24] H. M. McCormack, J. d. L. David, and S. Sheather, "Clinical applications of visual analogue scales: A critical review", *Psychological medicine*, vol. 18, no. 4, pp. 1007–1019, 1988.
- [25] S. M. Phillips, R. Thompson, and J. L. Oliver, "Overestimation of required recovery time during repeated sprint exercise with self-regulated recovery", *The Journal of Strength & Conditioning Research*, vol. 28, no. 12, pp. 3385–3392, 2014.
- [26] A. Savitzky and M. J. Golay, "Smoothing and differentiation of data by simplified least squares procedures.", *Analytical chemistry*, vol. 36, no. 8, pp. 1627–1639, 1964.

- [27] J. Fox and S. Weisberg, *An R companion to applied regression*. Sage Publications, 2018.
- [28] S. Jaric, D. Ugarkovic, and M. Kukoli, "Evaluation of methods for normalizing muscle strength in elite and young athletes", *Journal of Sports Medicine and Physical Fitness*, vol. 42, no. 2, p. 141, 2002.
- [29] M. H. Stone, W. A. Sands, J. Carlock, S. Callan, D. Dickie, K. Daigle, J. Cotton, S. L. Smith, and M. HARTMAN, "The importance of isometric maximum strength and peak rate-of-force development in sprint cycling", *The Journal of Strength & Conditioning Research*, vol. 18, no. 4, pp. 878–884, 2004.
- [30] M. Efronymson, "Multiple regression analysis", *Mathematical methods for digital computers*, pp. 191–203, 1960.
- [31] S. S. Shapiro and M. B. Wilk, "An analysis of variance test for normality (complete samples)", *Biometrika*, vol. 52, no. 3/4, pp. 591–611, 1965.
- [32] H. Lorås, S. Leirdal, and G. Ettema, "Force effectiveness during cycling at different pedalling rates", *J Appl Biomech*, vol. 25, pp. 85–92, 2009.
- [33] T. Henke, "Real-time feedback of pedal forces for the optimization of pedaling technique in competitive cycling", in *ISBS-Conference Proceedings Archive*, vol. 1, 1998.
- [34] L. Rylands, S. J. Roberts, M. Cheetham, and A. Baker, "Velocity production in elite bmx riders: A field based study using a srm power meter", 2013.
- [35] L. P. Rylands, S. J. Roberts, H. T. Hurst, and I. Bentley, "Effect of cadence selection on peak power and time of power production in elite bmx riders: A laboratory based study", *Journal of sports sciences*, vol. 35, no. 14, pp. 1372–1376, 2017.
- [36] P. D. Allison, *Multiple regression: A primer*. Pine Forge Press, 1999.
- [37] M. Fisher and L. J. Wills, *Crank arm with strain amplifier*, US Patent 8,584,529, Nov. 2013.
- [38] P. Barratt, "Kinetics of sprint cycling with a below-knee prosthetic limb: A case study of a paralympic champion", in *ISBS-Conference Proceedings Archive*, vol. 1, 2011.
- [39] H. P. Giorgi, M. H. Andrews, A. J. Gray, and M. A. Osborne, "An updated approach to incremental cycling tests: Accounting for internal mechanical power", *Journal of Science and Cycling*, vol. 4, no. 1, p. 33, 2015.
- [40] C. P. Earnest, R. P. Wharton, T. S. Church, and A. Lucia, "Reliability of the lode excalibur sport ergometer and applicability to computrainer electromagnetically braked cycling training device", *The Journal of Strength & Conditioning Research*, vol. 19, no. 2, pp. 344–348, 2005.

Appendix A

Description and specifications of the instrumented cranks

A.1 Product description

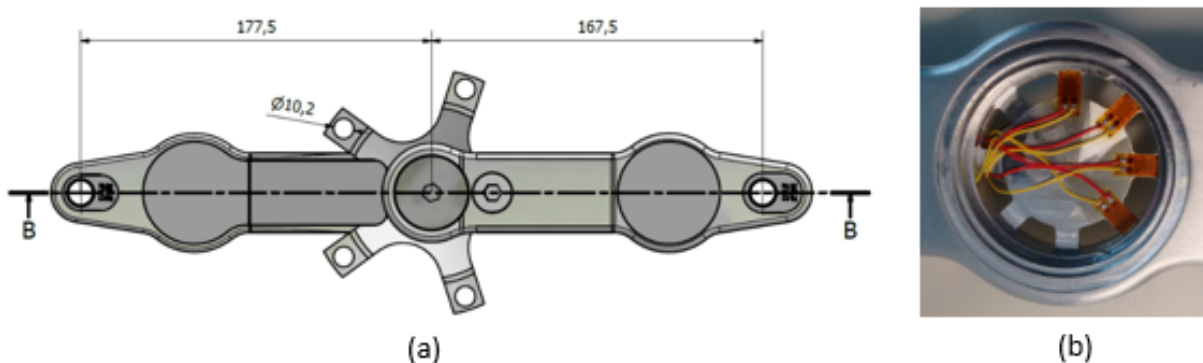


Figure A.1: Swift performance Axis2 power meter schematic drawing (a) shows a circular expansion of the crank arms. Within this circular expansions there is a mechanical amplifier with strain gauge for the measurement of the radial force (b).

Swift performance manufactured the Axis2 measurement system Figure A.1. The device uses strain gauge method in full Wheatstone configuration to measure strain in a metal crank arm. According to the patent a direct application of strain sensing would require a signal amplification by 3500 to have a processable signal, this gain would be difficult to achieve while maintaining low power, low thermal drift and low noise [37]. The star shape (Figure A.1 (b)) is a incorporated mechanical strain amplifier which solves this issue by making the radial force measurement 40 time more sensitive. This means an amplified of only 90 would be required to generate a accurate signal, which are widely commercially available. The cranks can set to a sample frequency of 100, 200 or 400 Hz, the crank angular velocity has a maximum of 200Hz, the Bluetooth transmission to a laptop has a limited sample frequency of 100Hz. The radial force range is $\pm 2500N$ and crank torque range is $\pm 500Nm$. This system has been used in literature during short (4s) seated maximal sprint on a isokinetic ergometer (SRM, Julich, Germany) [38] and assessment of negative crank power during the upstroke to describe the transfer of power between external (EP) and internal (IP) mechanical power [39]. No

academic research has been found reporting on validity and reproducibility of the Axis2D system. Unpublished internal tests conducted by ergometer manufacturer Lode (Lode B.v., Groningen, The Netherlands) found that the results did correlate with those obtained from the Excalibur sport with Pedal Force Measurement (PFM). The Excalibur ergometer from Lode are renowned as “the gold standard in ergometry” for its reliability [40] and is widely used as reliable ergometer in sport medicine for performance monitoring and rehabilitation.

A.2 Gain and Offset compensation

The instrumented cranks were pre-calibrated by the manufacturer, calibration setting provided in Table A.2. Twist compensation was also done by the manufacturer according to the following formula:

$$\begin{aligned}
 R_{comp} = & K0 + K1 \cdot R_c + K2 \cdot T_c + K3 \cdot R_c \cdot R_c + \\
 & K4 \cdot T_c \cdot T_c + K5 \cdot R_c \cdot T_c + K6 \cdot R_c \cdot R_c \cdot R_c + \\
 & K7 \cdot T_c \cdot T_c \cdot T_c + K8 \cdot R_c \cdot R_c \cdot T_c + K9 \cdot R_c \cdot T_c \cdot T_c
 \end{aligned} \tag{A.1}$$

where R_{comp} is the compensated radial value (N), R_c the calibrated radial value before compensation (N), T_c the calibrated tangential value (Nm) and $K0 - 9$ the coefficients as per table A.1

Left		Right	
Coeff.	Value	Coeff.	Value
K0	2.72476196289063	K0	-8.81728076934814
K1	1.01236021518707	K1	1.00932705402374
K2	0.457647383213043	K2	0.194752633571625
K3	-0.0173586704477202E-3	K3	-7.17702141628251E-06
K4	5.14142960309982E-3	K4	2.58165528066456E-3
K5	-0.253309000981972E-3	K5	0.205469244974665E-3
K6	-2.65569322088766E-09	K6	2.6415925002965E-09
K7	1.10663802388444E-06	K7	0.290532284452638E-06
K8	0.563651667562226E-06	K8	0.483340556911571E-06
K9	-0.457999988157098E-06	K9	0.600000021222513E-07

Table A.1: Twist compensation coefficients $K0 - 9$ for left and right crank

Left				Right			
Bits	Nm	Bits	N	Bits	Nm	Bits	N
8288	151.48	-9367	-1186.1	7920	151.14	-10416	-1234.9
-8967	-163.8	10868	1167.4	-8785	-170.44	10295	1183.5
6836	125.09	-7910	-996.4	5981	113.72	-8328	-965.5
-7630	-139.22	9211	990	-6996	-135.91	8106	937.5
5286	96.42	-6272	-784.2	4871	92.21	-6994	-794.2
-6124	-111.59	7309	786.3	-5787	-113.4	6612	768.7
3919	71.32	-4815	-591.8	3593	67.67	-5556	-606.8
-4737	-86.31	5562	601.6	-4408	-88.83	4888	587.8
3102	56.49	-3937	-479	2983	55.63	-4709	-504.4
-3914	-71.36	4527	491.5	-3832	-75.27	3994	487.8
2437	44.09	-3195	-378.5	2629	48.85	-4246	-445.6
				-3444	-67.8	3482	431.2
1511	27.08	-2269	-252.2	2210	40.72	-3740	-380.5
-2319	-42.24	2428	274.8	-2981	-58.94	2888	366.8
385	6.6	-1101	-94.9	545	9.07	-1894	-147.1
-1112	-20.4	871	117.7	-1337	-27.54	829	144.6

Table A.2: Calibration settings crankset

A.3 Data processing

Crank data was send wireless over a 2.4 GHz RF signal to a Analog Interface Receiver (AIR, Swift Performance) from where the crank data was forwarded via a Bluetooth 2.1 connection to a laptop running the provided crank user interface (AXIS v1.9.1, Swift Performance). Hardware specifications provided in table A.3 Via the crank user interface crank data was stored for every trial to a CSV file.

	Cranks (Left and Right)	Receiver (AIR)
Microprocessor	32 bit M0 Processor and ADC 12 bit absolute	32 bit M0 Processor and ADC 12 bit absolute
Communication	output: 16 bit over-sampled Radio-Propriety ISM band 2.4GHZ	input: 16 bit over-sampled Radio-Propriety ISM band 2.4GHZ. output: digital Bluetooth 2.1, analog BNC connectors
Power	400mAh Lipo- rechargeable ADC 12 bit absolute	7V DC 200mA plug pack

Table A.3: Hardware specifications on Axis2D instrumented cranks

Appendix B

Wheel velocity sensor

B.1 Hardware

The custom wheel velocity sensor (Figure B.1 consists of six components:

1. Sensor: NXP Precision 9DoF Breakout board
2. Development board: ARDUINO MKRZero
3. Storage: Micro SD card
4. Battery: Polymer Lithium Ion Battery - 2000mAh
5. I/O switch
6. Hub connection: 4mm elastic with hook

The NXP Precision 9DoF Breakout board has two sensors The FXOS8700 3-Axis accelerometer and magnetometer, and the FXAS21002 3-axis gyroscope. Only the FXAS21002 3-axis gyroscope data is stored for the purpose of a wheel velocity sensor, it is very precise as it has a zero-rate level of only 3.125 dps at $\pm 2000dps$ making one of the best in its kind (source: <https://learn.adafruit.com/comparing-gyroscope-datasheets/overview>). Moreover the FXAS21002 sensor has a Full-Scale Range boost function enabling a range of $\pm 4000dps$ by setting `CTRL_REG3 [FS_DOUBLE] = 1` and an angular rate sensitivity of $0.125^\circ/s$ at that range.

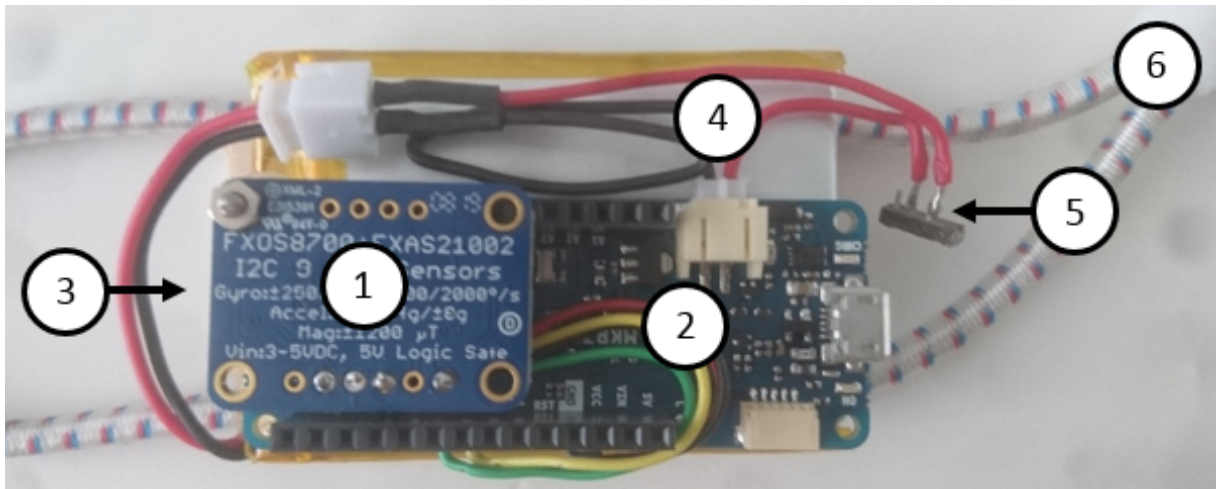


Figure B.1: Custom speed sensor (200Hz, range $\pm 4000^\circ/s$). The NXP Precision 9DoF Breakout board (1) has two sensors: The FXOS8700 3-Axis accelerometer and magnetometer, and the FXAS21002 3-axis gyroscope. The ARDUINO MKRZero (2) reads out the FXAS21002 3-axis gyroscope and data is logged on a Micro SD card (3). Power is supplied with a LiPo battery (4) and the power I/O switch (5) is used to create a new log file. An elastic band (6) secures the angular velocity sensor to the wheel hub.

B.2 Software

Arduino script showed below running on the MKRzero board to read out the gyroscope sensor and log data on the micro SD card (script composed from different example scripts). The gyroscope was set to an output data rate of 800Hz and full-scale range of $\pm 4000dps$. Data logging to the SD card was done at 200Hz, creating a CSV file with timestamp for every log reading in milliseconds.

```

1 #include <Wire.h>
2 #include <SD.h>
3 #include <Adafruit_Sensor.h>
4 #include <Adafruit_FXAS21002C.h>
5 #include "RTCLib.h"
6
7 const int chipSelect = SS1;
8
9 // the logging file
10 File logfile;
11
12 void error(char *str)
13 {
14   Serial.print("error:");

```



```
15  Serial.println(str);
16
17  while(1);
18 }
19
20 // how many milliseconds between grabbing data and logging it. 1000
    ms is once a second
21 #define LOG_INTERVAL 5 // mills between entries (reduce to take more
    /faster data)
22
23 // how many milliseconds before writing the logged data permanently
    to disk
24 // set it to the LOG_INTERVAL to write each time (safest)
25 // set it to 10*LOG_INTERVAL to write all data every 10 datareads,
    you could lose up to
26 // the last 10 reads if power is lost but it uses less power and is
    much faster!
27 #define SYNC_INTERVAL 20*LOG_INTERVAL // mills between calls to flush
    () - to write data to the card
28 uint32_t syncTime = 0; // time of last sync()
29
30 #define ECHO_TO_SERIAL 1 // echo data to serial port
31
32 /* Assign a unique ID to this sensor at the same time */
33 Adafruit_FXAS21002C gyro = Adafruit_FXAS21002C(0x0021002C);
34
35 void displaySensorDetails(void)
36 {
37   sensor_t sensor;
38   gyro.getSensor(&sensor);
39   Serial.println("-----");
40   Serial.print ("Sensor:_____"); Serial.println(sensor.name);
41   Serial.print ("Driver_Ver:___"); Serial.println(sensor.version);
42   Serial.print ("Unique_ID:_____0x"); Serial.println(sensor.sensor_id
    , HEX);
43   Serial.print ("Max_Value:_____"); Serial.print(sensor.max_value);
    Serial.println("_rad/s");
44   Serial.print ("Min_Value:_____"); Serial.print(sensor.min_value);
    Serial.println("_rad/s");
```

```
45 Serial.print ("Resolution:___"); Serial.print(sensor.resolution);
    Serial.println("_rad/s");
46 Serial.println("-----");
47 Serial.println("");
48 delay(500);
49 }
50
51 void setup(void)
52 {
53   Serial.begin(9600);
54
55   /* Wait for the Serial Monitor */
56   //while (!Serial) {
57   //delay(1);
58   //}
59
60   Serial.println("Gyroscope_Test"); Serial.println("");
61
62   /* Initialise the sensor */
63   if(!gyro.begin())
64   {
65     /* There was a problem detecting the FXAS21002C ... check your
        connections */
66     Serial.println("Oops, _no_FXAS21002C_detected_..._Check_your_
        wiring!");
67     while(1);
68   }
69
70   Serial.print("Initializing_SD_card...");
71
72   // see if the card is present and can be initialized:
73   if (!SD.begin(chipSelect)) {
74     Serial.println("Card_failed,_or_not_present");
75     // don't do anything more:
76     while (1);
77   }
78   Serial.println("card_initialized.");
79
80   /* Display some basic information on this sensor */
```

```
81 displaySensorDetails();
82
83 // create a new file
84 char filename[] = "LOGGER00.CSV";
85 for (uint8_t i = 0; i < 100; i++) {
86     filename[6] = i/10 + '0';
87     filename[7] = i%10 + '0';
88     if (! SD.exists(filename)) {
89         // only open a new file if it doesn't exist
90         logfile = SD.open(filename, FILE_WRITE);
91         break; // leave the loop!
92     }
93 }
94
95 if (! logfile) {
96     error("couldnt_create_file");
97 }
98
99 Serial.print("Logging_to:_");
100 Serial.println(filename);
101
102 logfile.println("millis,x,y,z");
103 }
104
105 void loop(void)
106 {
107
108     // delay for the amount of time we want between readings
109     delay((LOG_INTERVAL -1) - (millis() % LOG_INTERVAL));
110
111     // log milliseconds since starting
112     uint32_t m = millis();
113     logfile.print(m);           // milliseconds since start
114     logfile.print(",_");
115 #if ECHO_TO_SERIAL
116     Serial.print(m);           // milliseconds since start
117     Serial.print(",_");
118 #endif
119 }
```

```
120  /* Get a new sensor event */
121  sensors_event_t event;
122  gyro.getEvent(&event);
123
124  logfile.print(event.gyro.x);
125  logfile.print(",_");
126  logfile.print(event.gyro.y);
127  logfile.print(",_");
128  logfile.print(event.gyro.z);
129  #if ECHO_TO_SERIAL
130  Serial.print(event.gyro.x);
131  Serial.print(",_");
132  Serial.print(event.gyro.y);
133  Serial.print(",_");
134  Serial.print(event.gyro.z);
135  #endif //ECHO_TO_SERIAL
136
137  logfile.println();
138  #if ECHO_TO_SERIAL
139  Serial.println();
140  #endif // ECHO_TO_SERIAL
141
142  // Now we write data to disk! Don't sync too often - requires 2048
    bytes of I/O to SD card
143  // which uses a bunch of power and takes time
144  if ((millis() - syncTime) < SYNC_INTERVAL) return;
145  syncTime = millis();
146
147  logfile.flush();
148 }
```

Appendix C

Figures of results

C.1 Cumulative work figures

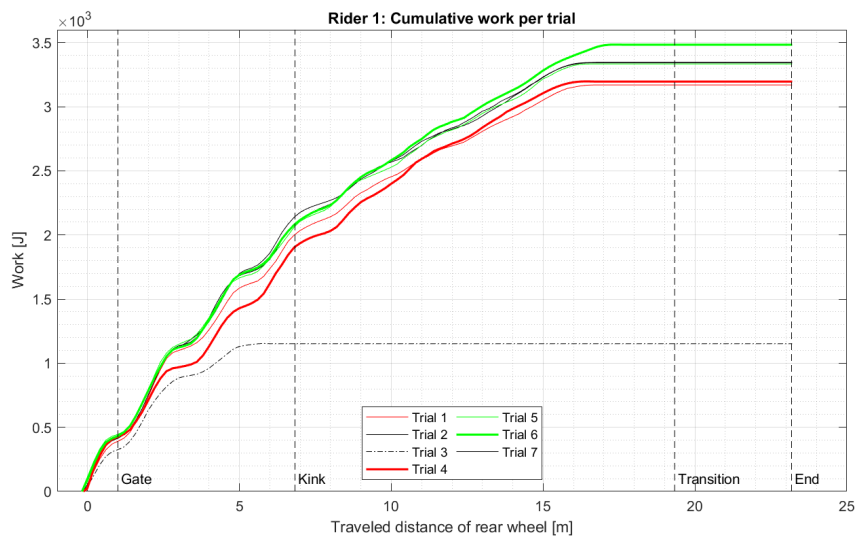


Figure C.1: Cumulative work done by rider 1 for every trial over the traveled distance on the start ramp. In red (Trial 1 and 4) the two slowest start times (t_{end}) in which the bold line is the slowest trial (Trial 4), in green (Trial 5 and 6) the two fastest start times in which the bold line is the fastest trail (Trial 6). Trial 3 (black dashed point line) was discontinued prematurely by the rider because of hitting the gate with the front wheel, therefore trial 3 is excluded in further analysis. 0 m is the contact point between the rear wheel and the ramp. The horizontal line at end of the ramp means no added work over that distance, i.e. stopped pedaling at the end of the ramp to prepare for jump.

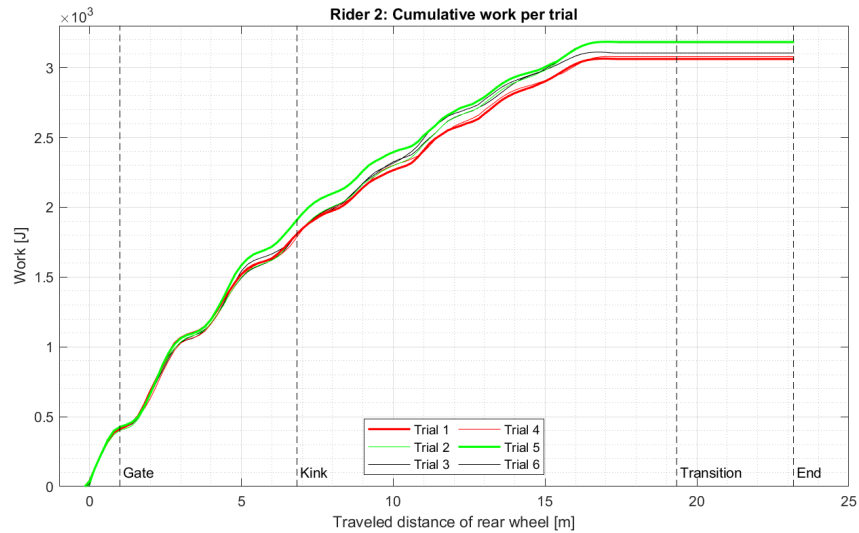


Figure C.2: Cumulative work done by rider 2 for every trial over the traveled distance on the start ramp. In red (Trial 1 and 4) the two slowest start times (t_{end}) in which the bold line is the slowest trial (Trial 1), in green (Trial 2 and 5) the two fastest start times in which the bold line is the fastest trail (Trial 5). The horizontal line at end of the ramp means no added work over that distance, i.e. stopped pedaling at the end of the ramp to prepare for jump.



Figure C.3: Cumulative work done by rider 3 for every trial over the traveled distance on the start ramp. In red (Trial 1 and 2) the two slowest start times (t_{end}) in which the bold line is the slowest trial (Trial 1), in green (Trial 5 and 6) the two fastest start times in which the bold line is the fastest trail (Trial 5). The horizontal line at end of the ramp means no added work over that distance, i.e. stopped pedaling at the end of the ramp to prepare for jump.

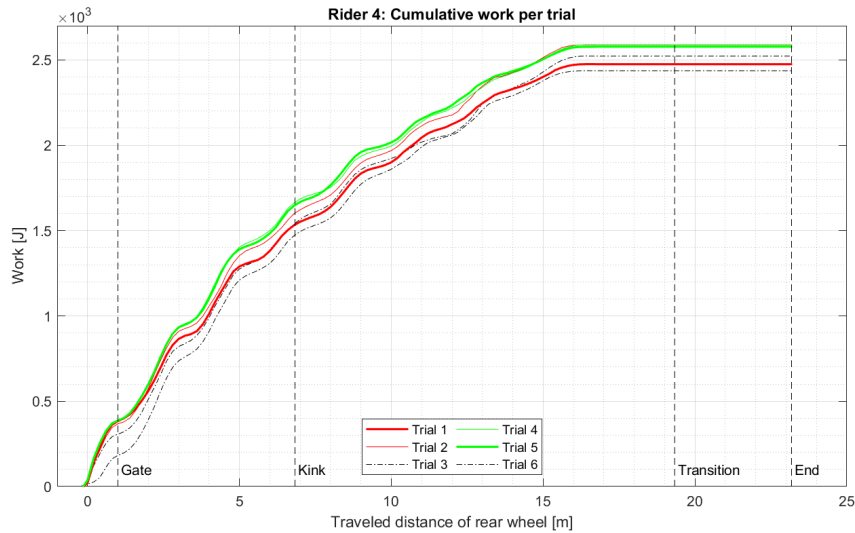


Figure C.4: Cumulative work done by rider 4 for every trial over the traveled distance on the start ramp. In red (Trial 1 and 2) the two slowest start times (t_{end}) in which the bold line is the slowest trial (Trial 1), in green (Trial 4 and 5) the two fastest start times in which the bold line is the fastest trail (Trial 6). Trial 3 and 6 (black dashed point line) were excluded for further analysis due to missed data of the link crank during wireless transmission. 0 m is the contact point between the rear wheel and the ramp. The horizontal line at end of the ramp means no added work over that distance, i.e. stopped pedaling at the end of the ramp to prepare for jump.

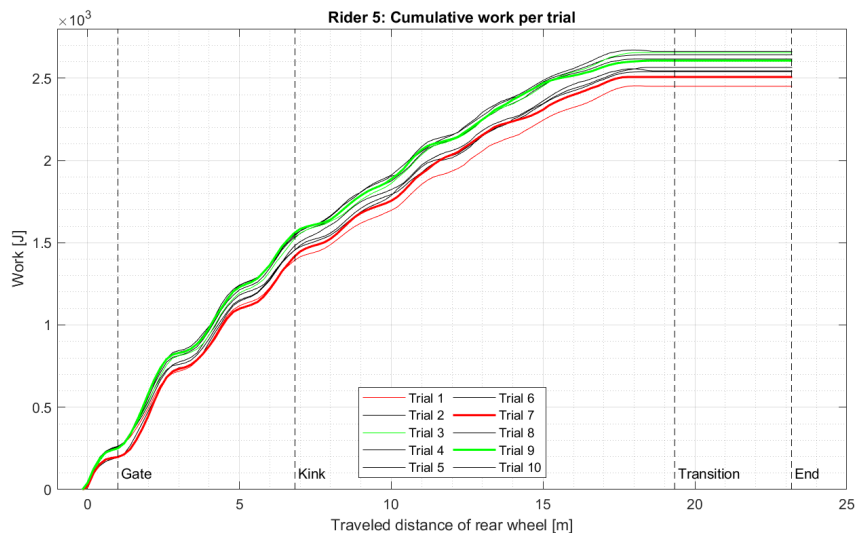


Figure C.5: Cumulative work done by rider 5 for every trial over the traveled distance on the start ramp. In red (Trial 1 and 7) the two slowest start times (t_{end}) in which the bold line is the slowest trial (Trial 7), in green (Trial 3 and 9) the two fastest start times in which the bold line is the fastest trail (Trial 9). The horizontal line at end of the ramp means no added work over that distance, i.e. stopped pedaling at the end of the ramp to prepare for jump.

Appendix D

Regression model details

General variables absolute data:

$$t_{start} = 2.8898 - 0.038113 \cdot V_i - 7.4029 \cdot 10^{-5} \cdot P_{max} \quad (D.1)$$

With model performance parameters: $RMSE = 0.274$, $R^2_{Adj} = 0.845$, p-value = $7.43 \cdot 10^{-11}$. Shapiro-Wilk normality test gives a p-value of 0.4771, which is well above 0.05. Details of the model are presented in table D.1 and Figure D.1.

	Coeff.	SE	tStat	pValue
Intercept	2.8898	0.032682	88.421	1.09E-31
V_i	-0.03811	0.01324	-2.8787	0.008263
P_{max}	-7.40E-05	1.15E-05	-6.4206	1.2227E-06

Table D.1: Multiple regression analyses of general independent variable effects on starting time. The intercept is the constant in the model, the expected mean value of starting time when all variables are zero.

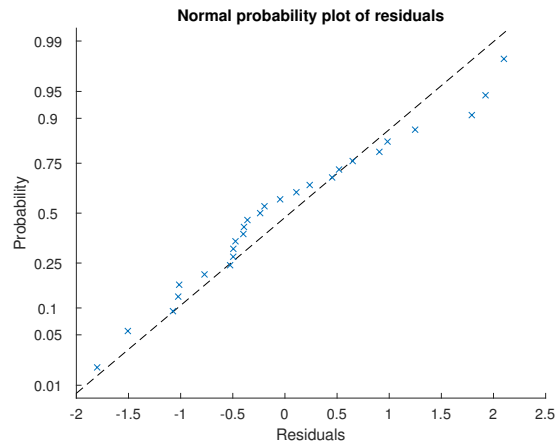


Figure D.1: Normal probability plot, General variables, Absolute power data. some departures from normality occur around zero and higher residual values

When choosing W_{top} over P_{max} the regression model becomes:

$$t_{start} = 3.1258 - 2.5877E-4 \cdot W_{top} \quad (D.2)$$

With model performance parameters: $RMSE = 0.0216$, $R_{Adj}^2 = 0.904$, p-value = $2.04 \cdot 10^{-14}$. Shapiro-Wilk normality test gives a p-value of 0.0266. Details of the model are presented in table D.2 and Figure D.2.

	Coeff.	SE	tStat	pValue
Intercept	3.1258	0.030608	102.12	2.71E-34
W_{top}	-2.5877E-04	1.6547E-05	-15.638	2.0377E-14

Table D.2: Multiple regression analyses of general independent variable effects on starting time using W_{top} . The intercept is the constant in the model, the expected mean value of starting time when all variables are zero

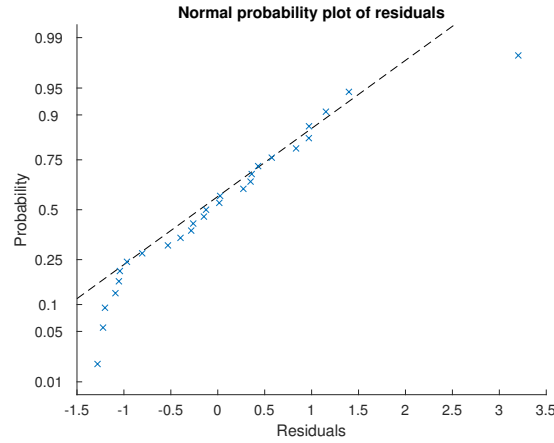


Figure D.2: Normal probability plot, General variables, Absolute work data. some departures from normality occur at the lower residual values, one outlier at high residual value.

General variables ratio scaled data: Using ratio scaled data, the regression equation becomes:

$$t_{start} = 3.1451 - 0.039527 \cdot V_i - 0.0041503 \cdot m_b - 0.0038815 \cdot P_{max} \quad (D.3)$$

With model performance parameters: $RMSE = 0.0255$, $R_{Adj}^2 = 0.867$, p-value = $7.9 \cdot 10^{-11}$. Shapiro-Wilk normality test gives a p-value of 0.919, which is well above 0.05. Details of the model are presented in table D.3 and Figure D.3.

	Coeff.	SE	tStat	pValue
Intercept	3.1454	0.065002	48.385	1.2E-24
V_i	-0.039527	0.013147	-3.0065	0.0062935
m_b	-0.0041503	0.77843E-3	-5.3316	2.0568E-5
P_{max}	-0.0038815	0.0016256	-2.3878	0.025555

Table D.3: Multiple regression analyses of ratio scaled general independent variable effects on starting time. The intercept is the constant in the model, the expected mean value of starting time when all variables are zero

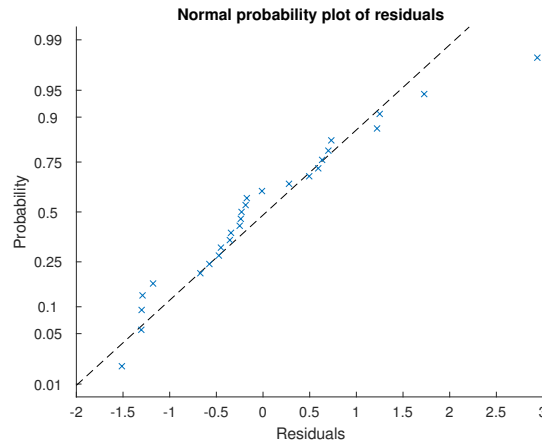


Figure D.3: Normal probability plot, General variables, Ratio scaled data. One outlier at high residual value.

Peddalling variables absolute data:

$$\begin{aligned}
 t_{start} = & 3.0666 - 0.033698 \cdot V_i - 1.0066 \cdot 10^{-4} \cdot L1Fe_{max} \\
 & - 7.4454 \cdot 10^{-5} \cdot T1Fe_{max} - 1.2137 \cdot 10^{-3} \cdot T1RMPD_{70}
 \end{aligned}
 \tag{D.4}$$

With model performance parameters: $RMSE = 0.0203$, $R^2_{Adj} = 0.915$, $p\text{-value} = 2.99 \cdot 10^{-12}$. Shapiro-Wilk normality test gives a $p\text{-value}$ of 0.1364, which is well above 0.05. Details of the model are presented in table D.4, and Figure D.4.

	Coeff.	SE	tStat	pValue
Intercept	3.0666	0.039186	98.26	2.08E-28
V_i	-0.033698	0.010892	-3.0938	0.0053
$L1-Fe_{max}$	-1.0066E-4	3.7151E-05	-2.7095	0.012802
$T1-Fe_{max}$	-7.4454E-5	3.1876E-5	-2.3357	0.029025
$T1-RMPD_{70}$	1.2137E-3	0.4256E-3	-2.8518	0.0092753

Table D.4: Multiple regression analyses of pedalling variable effects on starting time. The intercept is the constant in the model, the expected mean value of starting time when all variables are zero.

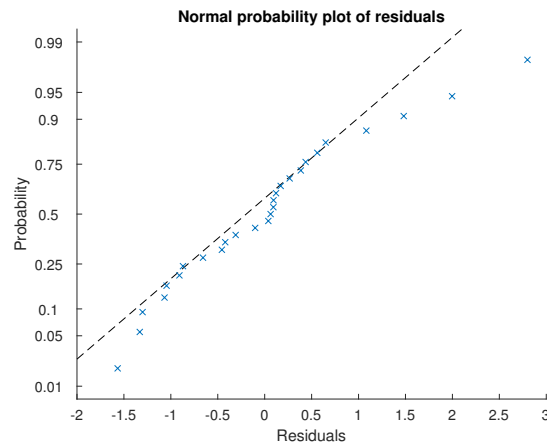


Figure D.4: Normal probability plot, pedalling variables, absolute data. Some departures from normality occur outside -1 and 1 for residual values.

Using power peak over effective force peak, the regression equation becomes:

$$\begin{aligned}
 t_{start} = & 3.0205 - 0.033357 \cdot V_i - 5.5069 \cdot 10^{-5} \cdot L1P_{max} \\
 & - 5.2495 \cdot 10^{-5} \cdot T1P_{max} - 1.5549 \cdot 10^{-3} \cdot T1RMPD_{70}
 \end{aligned}
 \tag{D.5}$$

With model performance parameters: $RMSE = 0.0183$, $R^2_{Adj} = 0.931$, $p\text{-value} = 3.14 \cdot 10^{-13}$. Shapiro-Wilk normality test gives a $p\text{-value}$ of 0.7596, which is well above 0.05. Details of the model are presented in table D.5 and Figure D.5.

	Coeff.	SE	tStat	pValue
Intercept	3.0205	0.043042	70.175	2.2699E-27
V_i	-0.033357	0.0095928	-3.4773	0.002375
$L1-P_{max}$	-5.5069E-5	1.3386E-05	-4.1139	0.45679E-3
$T1-P_{max}$	-5.2495E-5	1.6167E-5	-3.2471	0.0036974
$T1-RMPD_{70}$	1.5549E-3	0.39619E-3	-3.9246	0.72482E-3

Table D.5: Multiple regression analyses of pedalling variable, using power peaks, effects on starting time. The intercept is the constant in the model, the expected mean value of starting time when all variables are zero.

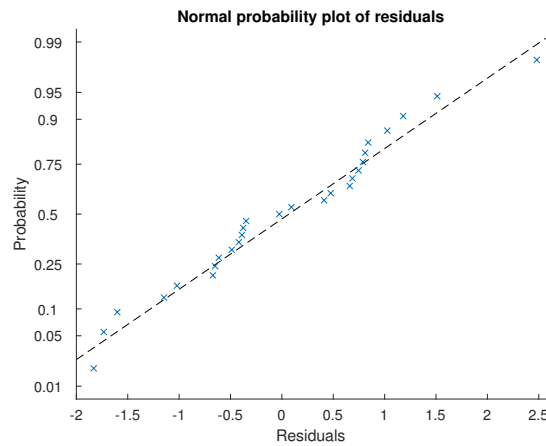


Figure D.5: Normal probability plot, pedalling variables, absolute data with power. Data seems to follow normality line well.

Pedalling variables ratio scaled data: Using ratio scaled data, using ratio scaled effective force peak the regression equation becomes:

$$t_{start} = 2.5649 - 0.039837 \cdot V_i - 0.0022431 \cdot T1RMPD_{70} + 0.44949 \cdot DC1 \quad (D.6)$$

With model performance parameters: $RMSE = 0.0259$, $R_{Adj}^2 = 0.862$, $p\text{-value} = 1.22 \cdot 10^{-10}$. Shapiro-Wilk normality test gives a $p\text{-value}$ of 0.4728, which is well above 0.05. Details of the model are presented in table D.6 and Figure D.6.

	Coeff.	SE	tStat	pValue
Intercept	2.5649	0.079884	32.107	1.3138E-20
V_i	-0.39837	0.014513	-2.745	0.011535
T1-RMPD ₇₀	-0.0022431	0.4601E-3	-4.8752	6.3581E-5
DC1	0.449495	0.10355	4.3406	0.24089E-3

Table D.6: Multiple regression analyses of ratio scaled pedalling variable, effects on starting time. The intercept is the constant in the model, the expected mean value of starting time when all variables are zero.

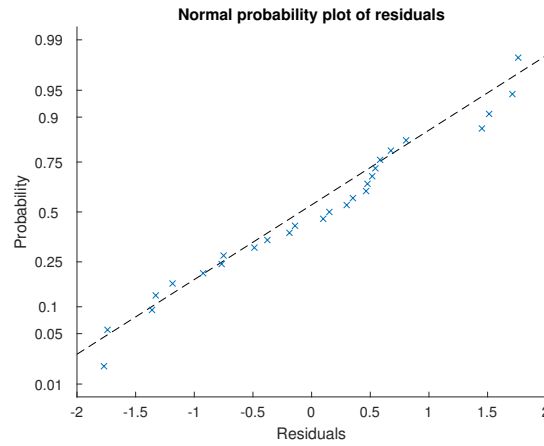


Figure D.6: Normal probability plot, pedalling variables, ratio data. Data seems to follow normality line well.

Using ratio scaled data, using ratio scaled power peak the regression equation becomes:

$$\begin{aligned}
 t_{start} = & 2.738 - 0.030117 \cdot V_i - 0.0051786 \cdot T1 - P_{max} \\
 & - 0.0017161 \cdot T1 - RMPD_{70} + 0.2914 \cdot DC1
 \end{aligned} \tag{D.7}$$

With model performance parameters: $RMSE = 0.0226$, $R_{Adj}^2 = 0.895$, $p\text{-value} = 2.96 \cdot 10^{-11}$. Shapiro-Wilk normality test gives a p-value of 0.3533, which is well above 0.05. Details of the model are presented in table D.7 and Figure D.7.

	Coeff.	SE	tStat	pValue
Intercept	2.738	0.091712	29.854	2.6954E-19
V_i	-0.030117	0.013068	-2.3047	0.030998
$T1-P_{max}$	-0.0051786	0.0017895	-2.8938	0.0084242
$T1-RMPD_{70}$	-0.0017161	0.43985E-3	-3.9015	0.76664E-3
DC1	0.2914	0.10538	2.7653	0.011289

Table D.7: Multiple regression analyses of ratio scaled pedalling variable, using power peaks, effects on starting time. The intercept is the constant in the model, the expected mean value of starting time when all variables are zero.

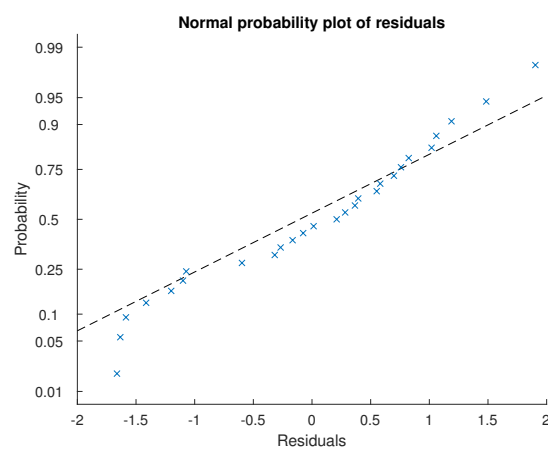


Figure D.7: Normal probability plot, pedalling variables, ratio data with power. Data seems to follow normality line well, some deviation below -1 and above 1.